forests

MDPI

Article

Modeling the Hydrological Regime of Litani River Basin in Lebanon for the Period 2009–2019 and Assessment of Climate Change Impacts Under RCP Scenarios

Georgio Kallas [1,2,†], Salim Kattar [2] and Guillermo Palacios-Rodríguez [3,*]

[1] Department of Landscape and Territory Planning, Faculty of Agriculture, Lebanese University, Beirut P.O. Box 6573/14, Lebanon; georgio.kallas@ul.edu.lb
[2] Department of Environment and Natural Resources, Faculty of Agriculture, Lebanese University, Beirut P.O. Box 6573/14, Lebanon; skattar@ul.edu.lb
[3] Laboratory of Forestry Digitalization and Development, ERSAF PAI RNM360 Research Group, Forest Engineering Department, University of Cordoba, 14071 Cordoba, Spain
* Correspondence: gpalacios@uco.es; Tel.: +34-957218381
† This manuscript is part of a PhD Thesis by the first author, available online at https://helvia.uco.es/handle/10396/22790 (accessed on 19 August 2025).

Abstract

This study investigates the combined impact of climate change and land use changes on water resources and soil conditions in the Litani River Basin (LRB) in Lebanon. The Mediterranean region, including the LRB, is highly vulnerable to climate change. This study utilizes the WiMMed (Water Integrated Management for Mediterranean Watersheds) model to assess hydrological variables such as *infiltration*, *runoff*, and *soil moisture* for the years 2009, 2014, and 2019. It considers 2019 climate conditions to project the 2040 scenarios for Representative Concentration Pathways (RCPs) 2.6 and 8.5, incorporating the unique characteristics of the Mediterranean watershed. Results indicate a concerning trend of declining *infiltration*, *runoff*, *and soil moisture*, particularly under the more severe RCP 8.5 scenario, with the most significant reductions occurring during summer. Land use changes, such as deforestation and urban expansion, are identified as key contributors to reduced *infiltration* and increased *runoff*. This study highlights the critical role of *soil moisture* in crop productivity and ecosystem health, showing how land cover changes and climate change intensify these effects. *Soil moisture* is highly sensitive to *precipitation* variations, with a 20% reduction in *precipitation* and a 5 °C temperature increase leading to substantial decreases in *soil moisture*. These findings highlight the urgent need for sustainable land management practices and climate mitigation strategies in the Litani River Basin (LRB) and similar Mediterranean watersheds. Protecting forests, implementing soil conservation measures, and promoting responsible urban development are crucial steps to maintain water resources and soil quality. Furthermore, this research offers valuable insights for policymakers, farmers, and environmentalists to prepare for potential droughts or flooding events, contributing to the preservation of this vital ecosystem. The data from this study, along with the recommended actions, can play a crucial role in fostering resilience at the national level, addressing the challenges posed by climate change.

Keywords: Litani River; Lebanon; watershed; hydrological modeling; climate change; future scenarios

check for updates

Academic Editor: Carlos R. Mello

Received: 12 April 2025
Revised: 5 August 2025
Accepted: 20 August 2025
Published: 13 September 2025

Citation: Kallas, G.; Kattar, S.; Palacios-Rodríguez, G. Modeling the Hydrological Regime of Litani River Basin in Lebanon for the Period 2009–2019 and Assessment of Climate Change Impacts Under RCP Scenarios. *Forests* **2025**, *16*, 1461. https://doi.org/10.3390/f16091461

Copyright: © 2025 by the authors. Licensee MDPI, Basel, Switzerland. This article is an open access article distributed under the terms and conditions of the Creative Commons Attribution (CC BY) license (https://creativecommons.org/licenses/by/4.0/).

1. Introduction

Climate change's future effects on water resources and soil conditions are highly negative. One of the most significant effects of this occurrence will be on local water resource availability, which will affect a variety of industries, including agriculture [1]. Increased greenhouse gas concentrations are expected to have a considerable impact on *precipitation*, *runoff* processes, and water supplies as a result of global warming [2]. Along with that, riverine ecosystems are among the most sensitive to climate change because they are directly linked to the hydrological cycle, closely dependent on atmospheric thermal regimes, and at risk from interactions between climate change and existing, multiple, and anthropogenic stressors [3,4]. Even though over the past 30 years warming trends have been consistently reported from global to regional scales, climate change is not in all cases the exclusive reason for this warming. Temporal trends in thermal regimes can also be influenced by anthropogenic pressures such as impoundment, water extraction, warm-water emissions from cooling and wastewater discharges, land use change (particularly deforestation), or river flow regulation.

Lebanon faces a complex and pressing challenge of water scarcity, climate change risks, and agricultural dependence in the Mediterranean region. The country, renowned for its rich history and cultural diversity, confronts a terrible water decline due to over-extraction, pollution, and shifting weather patterns intensified by climate change. This alarming confluence of factors threatens not only the nation's agricultural sector, a vital source of livelihood, but also its ecological balance, food security, and social stability, demanding urgent attention and sustainable solutions. Water supplies have fallen to 590 cubic meters per capita, significantly below the world average, exacerbated by climate impacts like prolonged droughts and irregular rainfall. These pressures demand urgent, sustainable solutions to address escalating socio-economic and environmental vulnerabilities.

The Mediterranean is considered a "hot spot" regarding its sensitivity to climate change, according to the most recent assessment from the International Panel on Climate Change [5]. Against a 1980 to 2000 baseline, mean surface temperatures are projected to climb 2.2 to 5.1 °C by 2080 to 2100 [6], while land *precipitation* may decrease by 4% to 27%. Irrigation demand could rise 4% to 18% from climate change alone and 22% to 74% when population growth is added [7]. Tourism, industrial expansion, and urban sprawl will worsen water pollution. Sea-water acidification, stronger heat waves, droughts, and land use change threaten ecosystems, biodiversity, and fisheries, already forcing shifts in agricultural and fishery yields. Many late-20th-century anomalies, such as glacier melt in Spain and Turkey and heat waves in Portugal, are attributed to global warming. By 2025, the region faces pressing challenges in energy, water, urban, and rural sectors [5].

The Middle East's dwindling water supplies are fueling tensions and conflicts [8]. River ecosystems respond to both environmental conditions and human activities [9], while riparian management must contend with complex hydro-physical and socio-economic–political interactions under deep uncertainty [10]. Lebanon's Litani River Basin (LRB) (the country's longest river at over 170 km, with an annual flow of 385 million m^3) is already facing severe aquifer drawdown [11], making groundwater unreliable. Urgent action is needed to protect vulnerable populations in polluted water areas [12], strengthen land cover management against scarcity, and ensure sustainable water availability through robust resource planning that accounts for hydrologic variability [13].

Hydrologic modeling is essential for forecasting seasonal water supply and guiding resource decisions [14], yet historical data for the LRB were once scarce. Recent years have seen major improvements in meteorological and pedological observations (2009–2019 remained stable [15]) and comprehensive studies that clarify basin characteristics. With land cover now the dominant factor in the water balance, we must quantify how *infiltration*,

runoff, and *soil moisture* vary before choosing management strategies [16]. *Infiltration*, which is the soil's ability to absorb and transmit water, reduces surface flow and pollutant spread, whereas *runoff* occurs when *precipitation* outpaces *infiltration* and exacerbates floods. And future *precipitation* is projected to decline [5].

This research applies a spatially and temporally explicit hydrologic model (the WiMMed (Water Management Model for the Mediterranean)) to predict watershed water balances accurately and address both current and future freshwater supply challenges. This hydrological model is designed to address the unique climatic and hydrological conditions prevalent in Mediterranean basins. It encompasses critical components of the hydrological balance, including *precipitation*, evapotranspiration, *runoff*, and *infiltration*. It is also effective for observing temporal and seasonal variations in semi-arid regions [17]. The WiMMed model has been applied and developed further in several studies, particularly in southern Spain and North Africa. These references highlight its flexibility in modeling various hydrological scenarios, including climate change impacts, land use changes, and water resource planning in semi-arid to arid Mediterranean environments [18]. Hydrological seasonality critically influences natural ecosystem stability. In the Mediterranean, climate change disrupts watershed behavior through rising temperatures, shifting *precipitation*, and increased extreme weather, compromising water resource balance. These alterations intensify droughts, reduce water availability, and elevate flooding risks, challenging watershed-dependent communities, agriculture, and ecosystems [19,20]. Sustainable water management adaptation is now urgent to mitigate far-reaching impacts on the region's hydrological systems. This paper specifically compares spatial distributions of hydrological variables under current and future climatic scenarios to analyze projected temperature and *precipitation* effects on *runoff*, *infiltration*, and *soil moisture* in the Litani River Basin.

The land cover maps for 2009, 2014, and 2019 were generated to improve our understanding of hydrological processes and to show how land use transformations affect *soil moisture* in the first and second layers [21,22]. Growing concerns about increased anthropogenic activities and associated greenhouse gas emissions suggest significant climate shifts this century [23], with major impacts on hydrological and biological systems [24]. Climate change manifests as (1) rising average temperatures, (2) altered rainfall patterns, and (3) higher sea levels. Global Circulation Models (GCMs) simulate present and future climates, providing estimates of air temperature, *precipitation*, incoming radiation, vapor pressure, and wind speed [25,26].

The main goal of this research is to apply the WiMMed model to derive hydrological variables representing the Litani River Basin's water balance in 2009, 2014, and 2019, analyze their variance, and assess soil-moisture sensitivity to land cover change and climate scenarios. The specific objectives are the following:

- Generate hydrological variables with WIMMed to characterize the water balance in the soil's unsaturated zones.
- Compare 2009, 2014, and 2019 land cover maps to identify changes in type and area.
- Investigate the relationship between soil-moisture measurements and land use changes, inferring impacts on the first and second soil layers. Use GCM outputs under Representative Concentration Pathways (RCP 2.6 and RCP 8.5) to explore potential effects of climate change on the basin's hydrological variables.

2. Materials and Methods

2.1. Description of the Study Area

With a catchment area of around 2150 km^2 [27], the Litani River, together with the Qaraoun Reservoir, is the biggest and most important hydrological basin in Lebanon. The Litani, Lebanon's longest and largest river, runs entirely within its borders (Figure 1). There

are fifteen rivers in Lebanon, as well as roughly 2000 important springs. The Litani River is fed by various perennial tributaries, primarily Berdawni, Ghzayel, Qib Elias, and Chtoura. The River Basin's diverse land cover, particularly agricultural, leaves it prone to a variety of pollution issues, including heavy metals, microorganisms, and nutrients. For decades, the Bekaa Plain, which encompasses the majority of the Litani River Basin (LRB), has been plagued by substantial water quality and quantity issues, threatening people's right to clean water, food security, and safety, putting sustainable agricultural methods at risk, and depleting the ecosystem. The Litani River Basin is extremely important to the Lebanese economy, with nearly one million people who live within the basin depending on it for their water needs. Locals' social lives and energy needs are strictly related to the basin conditions [28]. The river has reached its worst conditions ever, such that it is called a "dead river" [27]. The progressing degradation of its state is strictly related to factors such as a growing population, untreated wastewater discharge, climate change, low water productivity, and a range of unsustainable activities [29]. Some of the causal elements influencing the basin's health include bulk disposal of solid wastes on the riverbanks and the direct discharge of untreated sewage and industrial fluids, in addition to the water washed away from the agri-fields, contaminating the river as per the farmers in the watershed's surroundings, who also use the contaminated river to irrigate their land. As a result, bacterial and chemical contamination of water and sediments has grown widespread, surpassing international criteria [30,31].

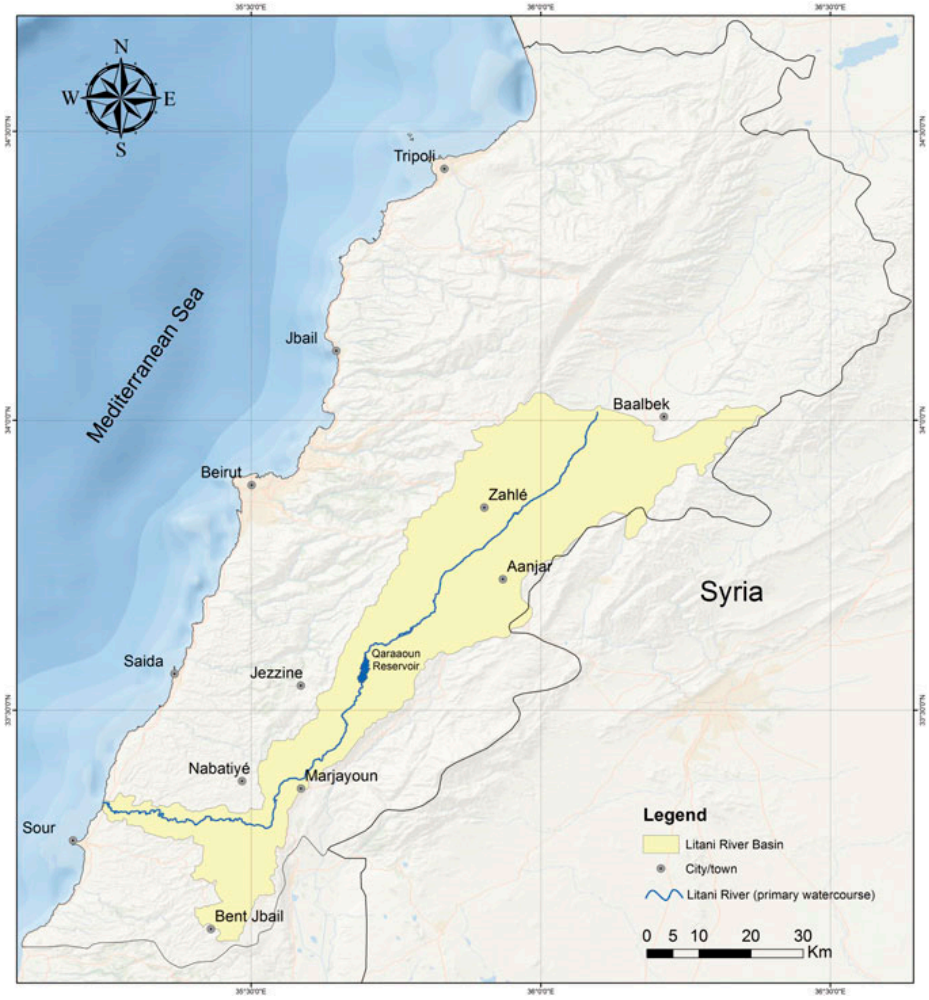

Figure 1. Location of the Litani River and its basin boundary [32].

2.2. Watershed Integrated Hydrological Model

2.2.1. Description of the Model

The WiMMed model (WiMMed 2021, University of Córdoba, Córdoba, Spain) was used in this work to compute all of the mechanisms that govern water flows throughout the watershed of the Litani Basin areas. This study analyzed the years 2009, 2014, and 2019, specifically corresponding to the periods 2009–2010, 2013–2014, and 2018–2019, because consistent datasets, including remote sensing-derived land cover maps and validated meteorological and hydrological data, were available.

For simplicity, these periods are referred to as 2009, 2014, and 2019. They encompass a decade at roughly five-year intervals, facilitating analysis of medium-term alterations in land cover and hydrological dynamics. Selection was not influenced by specific climate anomalies, but the distribution allows assessment of interannual variability and model responsiveness. Comparing different hydrological variables across years and seasons will evaluate long-term climatic behavior and explain flood occurrence.

The model outputs depict the watershed's hydrological regime using the following: *snowfall* (mm), *precipitation* (mm), *infiltration* (mm), *runoff* (mm), first-layer *soil moisture* (mm), and second-layer *soil moisture* (mm). These five variables were estimated for summer, autumn, winter, and spring of the designated years.

WiMMed focuses on spatial interpolation of meteorological variables and physical modeling of water and energy balance (raster format). It accounts for Mediterranean watershed characteristics impacting spatiotemporal variability (torrential rainfall, semi-aridity, and high drought risk) and processes where topography significantly influences results [33]. It links GIS-based watershed representations with advanced algorithms to physically model energy and water balance.

WiMMed was chosen because it is recognized as the best technique for accurately calculating complex Mediterranean-specific mechanisms. Key reasons include the following: (1) regional expertise: designed for Mediterranean climate systems (semi-arid/arid climates, complex topography, and land-sea interactions); (2) high resolution: operated at 30 m spatial resolution (matching DEM/land cover data) and daily temporal resolution, capturing fine-scale hydrological responses; (3) comprehensive mechanisms: accounts for sea surface temperatures, atmospheric circulation, mountain influences; (4) validation/performance: rigorously validated against observational data; (5) policy relevance: supports informed climate decision-making. Its specialization, mechanism coverage, and scientific credibility make it invaluable for Mediterranean climate challenges [34].

WiMMed calculates all mechanisms determining water flows in the Litani River Basin, accommodating different time scales per process [34]. Using input data (Section 2.2.2), its implicit interpolation mechanisms are applied to all variables, yielding meteorological results. Derived findings are presented as maps (e.g., distributed *precipitation*, *infiltration*) or tables (e.g., point flow, spatially aggregated means). Spatial/temporal scales are study-defined [35].

The Litani River Basin was chosen for model development/validation due to its extreme heterogeneity (climate, soil, meteorology, vegetation, water sources, land use, and water demand), resulting from a steep topographic gradient (30 km coast-to-peak distance). Its topographic algorithms show promise for analyzing ungauged watersheds via DEM and serve as a practical water management tool transferable to other watersheds.

2.2.2. Input Data Required for Modeling

The study region experiences highly variable *precipitation* throughout the year due to the presence of four seasons and the influence of topographical variation. In the following, we will be investigating the comparison of the hydrological variables modeled for the

2040s under the RCP 2.6 and RCP 8.5 scenarios in the Litani River Basin, Lebanon, with the hydrological variables from 2019. We assume that the future land use will remain the same as the current land use map (2019 land use/land cover map).

The RCPs were chosen for this study to facilitate research on climate change impacts and relevant policy solutions. The RCPs cover the range of forcing levels associated with various emission scenarios as a whole [36]. The RCPs try to capture these future trends. They make predictions of how concentrations of greenhouse gases in the atmosphere will change in the future as a result of human activities. This study uses the method of estimating average annual changes in *precipitation* and temperature under RCP 2.6 and RCP 8.5 to adjust historic temperature and *precipitation* series by adding T for temperature values and multiplying the values by (1 + P/100) for *precipitation*.

At each cell (30 m) of the watershed's digital elevation model, a distributed water and energy balance needed to be implemented as a cascade of reservoirs (vegetation cover, snow cover, and vadose zone of the soil). In event situations (e.g., storms), calculations are conducted on a one-hour time step; in non-event situations, calculations should be made on a one-day time step [37]. Distinct simulation levels, as well as different groups of resulting variables in terms of spatial and temporal resolution, will be chosen. The Surface Cycle simulation, which calculates the water balance in the soil's unsaturated zone, was employed in this study. The model requires various variables and input parameters to complete this simulation [37]. Topography, meteorology, and soil characteristics are the three major groups of input data. A brief description of the data collected for the LRB watershed and its processing for model application is as follows:

- Topography: Because the WIMMED model requires only elevation data as its primary input, this study used a high-resolution digital elevation model (DEM) encompassing all necessary topographic characteristics. From this DEM, the model derived additional topographic variables, such as the slope, aspect, and flow direction, internally. In this way, the elevation data provided fully satisfy the model's topographic requirements. A digital elevation model (DEM) with a horizontal resolution of 30 m and a vertical precision of 1 m represents the topographic input data. The Earth Explorer DEM (https://earthexplorer.usgs.gov/) (accessed on 1 January 2021) was used as the input DEM. The DEM for this model's application was created using (Entity ID: SRTM1N34E036V3, Publication Date: 23 September 2014, Resolution: 1-ARC). Using the ArcGIS Pro application (ArcGIS Pro 2.8, Esri, Redlands, CA, USA and ArcGIS Desktop 10.8, Esri, Redlands, CA, USA), a resample from 26.2709 × 30.1783 m to 30 × 30 m was performed. The soil map was used to project this raster. The DEM raster of the entire Litani River Basin, in Lebanon, was then retrieved. The DEM determines the extent, coordinates, and precision (cell size) of all the other maps, both as the input and its corresponding output [32]. A spatial resolution of 30 × 30 was chosen because of the case study area dimension and the quality of the remote sensing images available (LAND-SAT) in the assessment of the vegetation cover. The model will calculate the rest of the topographic variables involved in the water balance after the DEM is introduced: slope, direction, and horizons [38].
- Meteorological data: The model obtained daily and hourly recordings of *precipitation*, mean, maximum, and lowest temperatures, solar radiation, wind speed, vapor pressure, and the atmosphere's emissivity. We obtained weather data for this study from the six local weather stations (Table 1) around the river, covering the period 2009 to 2019, which were given to us by the Lebanese Agricultural Research Institute (LARI). We brought the data into the model after changing it into the required ASCII files.txt format. We employed interpolation methods to fill in the gaps left by station closures and disruptions caused by conflict. The primary variables included daily *precipitation*,

minimum and maximum temperature, and reference evapotranspiration, which are required for the WiMMed model. On average, less than 5% of daily records per year were missing across all stations. To address these gaps, we applied the inverse distance weighting (IDW) interpolation method, using data from nearby stations (within a 30 km radius) with similar elevation and climate characteristics. This method was selected for its reliability in mountainous terrain and prior successful application in Mediterranean hydrological studies.

Table 1. Weather stations in Litani River Basin.

Weather Station	X (Longitude)	Y (Latitude)
Bar Elias	33.772579	35.883633
Hasbaya	33.427703	35.631393
Hawch ammiq	33.699705	35.820220
Kferden	33.991048	36.085832
Machghara	33.515467	35.681196
Tal Amara	33.851276	35.972005

- Soil data: For this study, we used soil data from two main sources: a soil shapefile from the National Council for Scientific Research (CNRS) in Lebanon and detailed information about soil properties from Darwish 2006 published map [39], such as soil texture, infiltration rates, water retention capacity, and hydraulic conductivity. These datasets meet the WIMMED model's needs for soil input when used together. The CNRS is the official body in charge of making soil characteristics maps in Lebanon. The 2006 version is still the most recent one. The physicochemical and hydraulic parameters of the soil were evaluated using Darwish 2006's map published 1:50,000 scale soil map of Lebanon [39], which included information on soil textures. This study found five different soil textures in the examined watershed: clay, clay loam, loam, sandy clay loam, and sandy loam. Saturated surface conductivity (mm/h), porosity ($m^3 \times m^{-3}$), Van Genuchten retention parameter (dimensionless) [39], saturation and residual moisture values ($cm^3 \times cm^{-3}$), and soil thickness of layers 1 and 2 were utilized to construct thematic maps for the examined river (mm). Using local soil data will improve the performance of the model in comparison to using other "global database" of soils. The soil map database contains detailed information on landforms, lithology, slope gradient, drainage conditions, surface stoniness, texture, soil depth, and thickness. The final soil categorization system is based on the US soil taxonomy, the revised FAO UNESCO legend, and the World Reference Base [40]. With the exception of soil thickness, which has been measured for all soil types in Lebanon and published with the soil map of Lebanon [39], all of these metrics have been calculated based on soil texture. Table 2 shows the ranges of saturated hydraulic conductivity (Ksat) and porosity for the USDA soil texture defined by Saxton and Rawls [41]. The Van Genuchten parameter (n), as well as the residual (Θr) and saturated (Θs) water contents for various soil textural classes, are presented in Table 3, which was compiled from the Unsaturated Soil Hydraulic Database (UNSODA) database [42]. Table S1 shows the results of soil thickness (upper layer 1 and lower layer 2) based on soil type. The Litani River Basin topography is highly variable, with elevations ranging from sea level to over 2600 m above sea level, creating distinct zones including steep mountainous terrain, gently sloping agricultural plains, and undulating southern hills [43]. This variation influences water flow, erosion, and agricultural potential. The basin's soils are equally diverse: fertile Vertisols and Calcisols dominate the Bekaa Valley, supporting intensive agriculture due to their clay-rich and deep profiles, while shallow, stony Leptosols, and Regosols prevail in the upland areas, limiting water

retention and increasing erosion risk [44]. Riparian zones host Fluvisols, which are moderately fertile but susceptible to seasonal flooding. Soil salinity and localized degradation, especially near Qaraoun Lake, further constrain land productivity [45]. These combined topographic and edaphic features strongly shape land use, hydrology, and environmental management strategies within the basin. Table 4 shows an overview of WIMMED model input variables and sources.

Table 2. Ranges of saturated hydraulic conductivity (Ksat) and porosity for the USDA soil textural classes [41].

USDA Soil Texture Class	Ksat (mm/h)	Porosity (m^3/m^3)
Sand	0.5091–0.3058	0.48–0.46
Loamy sand	0.4464–0.1683	0.47–0.44
Sandy loam	0.3553–0.0744	0.47–0.42
Loam	0.0271–0.1538	0.48–0.46
Silt loam	0.0402–0.2126	0.48–0.46
Silt	0.0425–0.1068	0.49–0.47
Sandy clay Loam	0.0128–0.0653	0.45–0.42
Clay loam	0.0122–0.0256	0.50–0.45
Silty clay loam	0.0183–0.0252	0.53–0.49
Sandy clay	0.0003–0.0088	0.46–0.43
Silty clay	0.0115–0.0118	0.55–0.50
Clay	0.0103–0.0056	0.56–0.46

Table 3. Van Genuchten parameter (n) including residual (Θr) and saturated (Θs) water content compiled from the UNSODA database [42].

Textural Class	Θr (cm^3/cm^3)	Θs (cm^3/cm^3)	n
Sand	0.058	0.37	3.19
Loamy sand	0.074	0.39	2.39
Sandy loam	0.067	0.37	1.61
Loam	0.083	0.46	1.31
Silt	0.123	0.48	1.53
Silt loam	0.061	0.43	1.39
Sandy clay Loam	0.086	0.40	1.49
Clay loam	0.129	0.47	1.37
Silty clay loam	0.098	0.55	1.41
Silty clay	0.163	0.47	1.39
Clay	0.102	0.51	1.20

Table 4. Overview of WIMMED model input variables, sources, and coverage.

Input Variable	Source	Resolution	Temporal Coverage	Notes
Topography	DEM (2014)	30 m	2014	Stable variable, applicable all years
Climate	6 Meteorological Stations	Daily	2009–2019	Continuous dataset covering all years
Land Cover/Use	CNRS Shapefile	1:10,000 scale	2009, 2014, 2019	Matches study years
Soil	CNRS & Darwish (2006)	1:20,000 scale	2006	Stable characteristics, applicable all years

- Geologic data: WIMMED needs mostly geological data to describe how groundwater interacts, such as the parameters of aquifers, their permeability, and their porosity. For this investigation, geological data came from CNRS-provided shapefiles and

was supplemented by the extensive soil dataset made by Darwish (2006). Even though the CNRS shapefile and Darwish's data did not show specific geological layers separately, they do show important geological features in a way that is good enough for modeling how groundwater and surface water interact in the WIMMED framework. The formations ranging from Mid-Jurassic to recent Quaternary deposits are exposed in the upper Litani basin. The Jurassic formations span from the Middle Jurassic to the Late Jurassic. They cover an area of 122 km^2 of the catchment area, out of which 3 km^2 are Basalts and volcanic tuff, while 119 km^2 are composed mainly of limestone rocks. The Cretaceous formations span from the Early Cretaceous to the Late Cretaceous. The Cretaceous formations cover an area of 633 km^2 in the catchment area, composed of sandstone, limestone, and shale. The catchment area has six outcropping formations of the Cretaceous period. The Tertiary and Quaternary formations span from Eocene to Recent deposits. The Tertiary and Quaternary formations cover an area of 712 km^2 in the catchment area, composed of limestone and alluvial/fluvial deposits. The catchment area has three outcropping formations of the Tertiary and Quaternary periods. The Quaternary unconsolidated deposits cover most of the Bekaa plain within the Litani River Basin. In the center, the basin consists of a mixture of gravels, sands, silts, and clay of various concentrations depending on the areas. The Quaternary deposits reach a thickness of more than 400 m in the study area. The Quaternary deposits cover 414 km^2 of the study area (Figure 2).

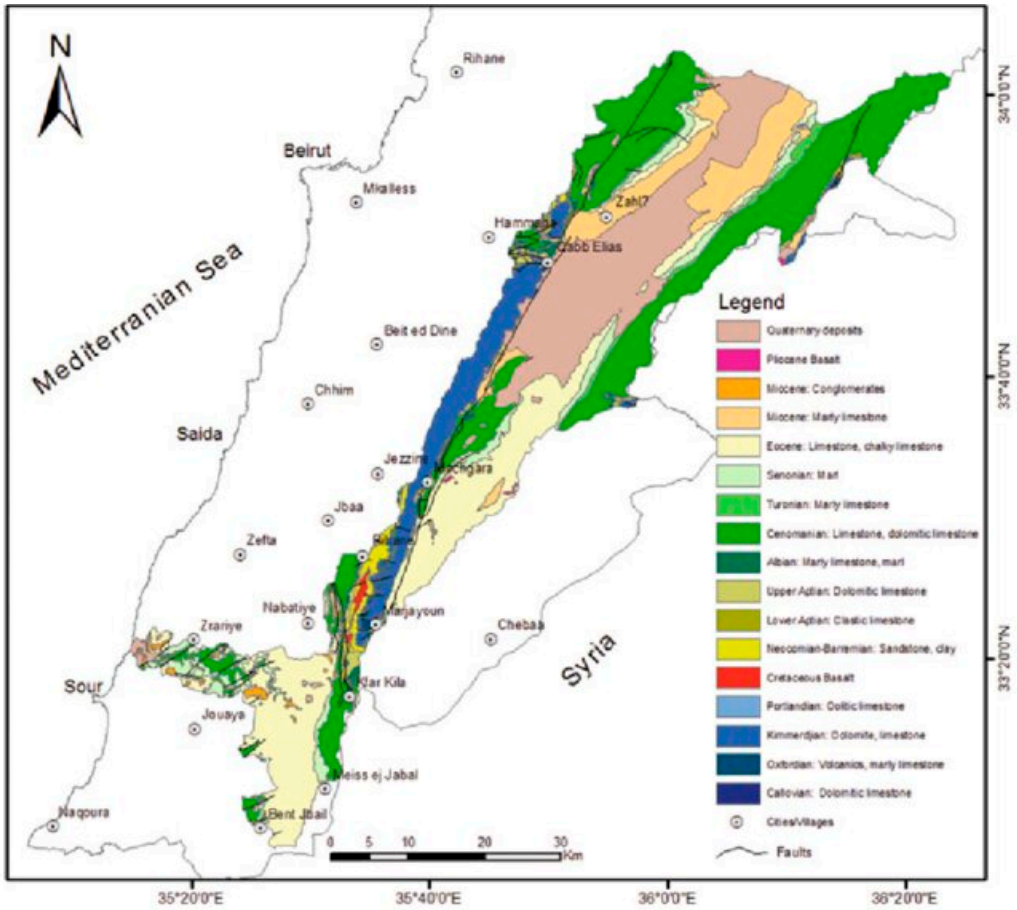

Figure 2. Geological map of the LRB [32].

2.2.3. Model Calibration

The calibration and validation of the WiMMed model for the Litani River Basin (LRB) could not be completed due to deficiencies in continuous hydrograph data. Despite these

constraints and limitations, significant efforts were made to guarantee the model's accuracy. The Litani River Authority (LRA) has preserved hydrological data since the 1960s, offering significant insights into the river's reaction to climatic and human factors. Nonetheless, considerable gaps and discrepancies remain in the observational dataset, mostly attributable to political instability, security-related operational interruptions, and institutional disturbances. *Runoff* values measured from the Guadalfeo River Basin in the Sierra Nevada Mountain range of southern Spain were utilized to address these data limitations. This decision was predicated on the similar hydrological attributes of the two basins. Both basins are mid-latitude Mediterranean mountainous systems in which *snowfall* substantially impacts the annual water balance. The WiMMed model was previously calibrated and validated satisfactorily in the Guadalfeo River Basin [38]. The parameters calibrated in that study were utilized to mimic hydrological conditions in the LRB (Table 5). Direct calibration with local observational data is optimal. However, transferring parameters from basins with analogous meteorological and physiographic conditions is a commonly endorsed approach in hydrological modeling when local data are scarce [46]. This methodology allowed the model to accurately replicate the observed patterns in *runoff* and *soil moisture* dynamics in the study area, taking into account existing land cover differences and anticipated climate scenarios. Despite this inherent limitation, the WiMMed model exhibited satisfactory performance, generating credible spatial and temporal hydrological patterns. This signifies its appropriateness for performing scenario assessments in the LRB. We acknowledge that future study would significantly benefit from improved field monitoring programs and enhanced data continuity, hence enabling more precise local calibration attempts.

Table 5. Calibration parameters used in WiMMed.

Soil Property	Parameter
Soil evaporation exponent	0.60
Soil evaporation coefficient	0.80

2.2.4. Summary of the Sources and Features of the Input Data (Table 4)

The WIMMED model employed data from national institutions that included important factors like terrain, climate, land cover, and soil. These datasets have different levels of spatial and temporal resolutions, but together they span the study period (2009–2019) consistently. Stable factors like terrain and soil were shown using high-resolution shapefiles along with reports from CNRS and Darwish (2006). Dynamic variables like climate and land use were shown using meteorological station data and CNRS land cover maps for the years 2009, 2014, and 2019.

3. Results

3.1. Physical Characteristics of the Study Area

The physical properties of the watershed, such as topography, weather, soil, and vegetation, are entered into the model as a preliminary stage of the hydrological studyThese administrative boundaries, managed by the Litani River Authority (LRA), represent the official management jurisdictions defined in accordance with Lebanese administrative decrees and policies. The study also present the entire hydrological catchment area of the Litani River (the administrative boundaries of the Bekaa, South, and Nabatiyeh governorates), delineated using geographic information systems (GIS). This representation highlights the direct influence that these administrative divisions have on the hydrological characteristics, management practices, and water resource governance of the Litani River and its tributaries.

3.1.1. Topography

The topography is specified by the research area's DEM (stereoscopic satellite image, USGS) (Figure 3). The slope gradients allow us to classify the mountains and obtain a sense of the diversity of landforms in the research area. The DEM shows that the highest altitudes (>2600 m) are found in the research area's northern and eastern regions. Lands with the lowest elevations (0 m) are found in the study area's southern and western regions, whereas lands with medium altitudes are found across the River Basin's center and western bounds.

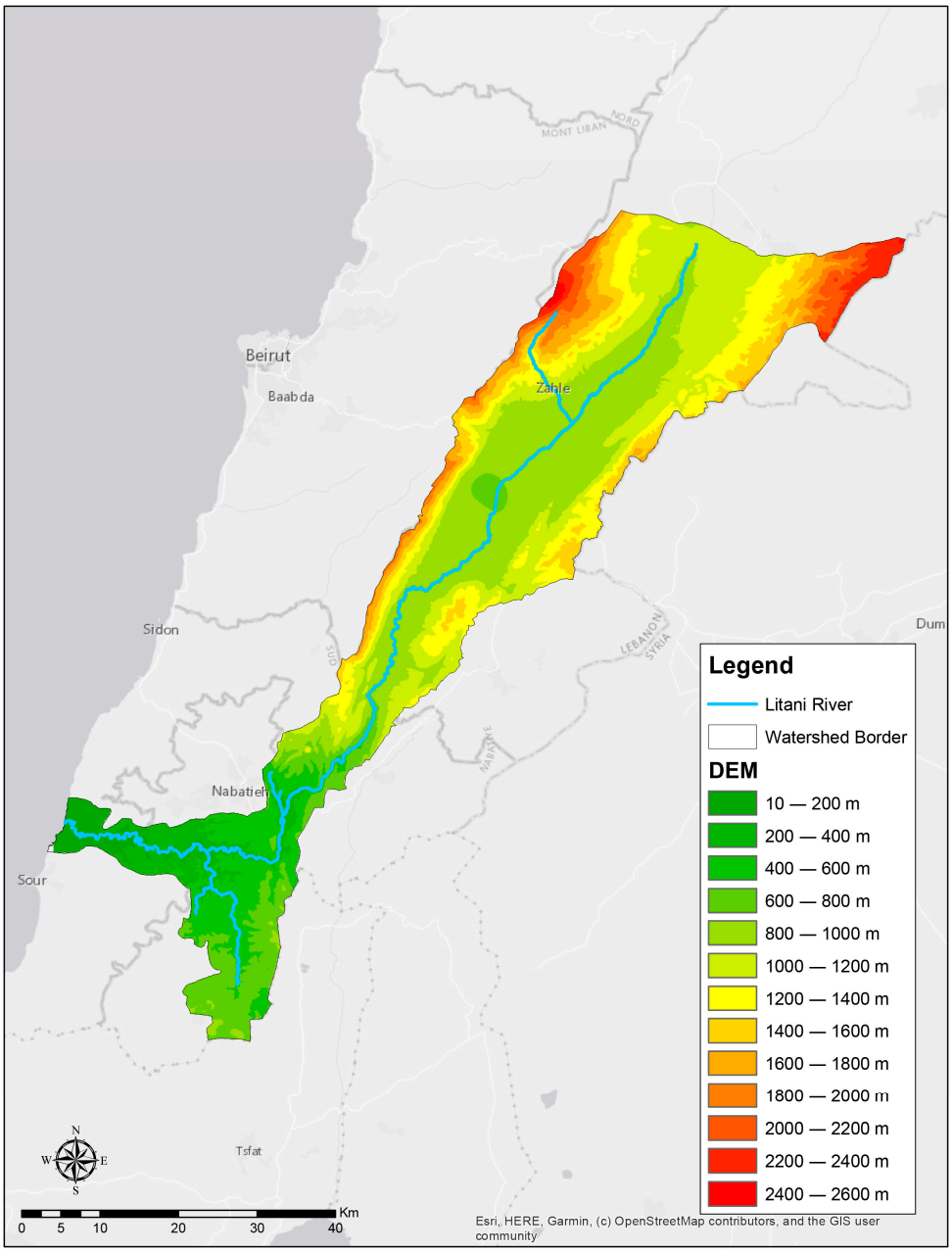

Figure 3. Digital elevation model of the study area.

3.1.2. Meteorology

According to the annual *precipitation* map (Figure 4), the Litani River Basin (LRB) experiences two main *precipitation* ranges. The upper parts of the basin receive annual *precipitation* between 1100 and 1200 mm, while the lower parts receive approximately 400 mm per year. Data from the six meteorological stations located in the study area

indicate that 2014 was significantly drier than 2009 and 2019, taking into account the minimum and maximum values recorded. A spatial analysis reveals a gradual expansion of areas receiving lower *precipitation* over time. Specifically, in 2009, regions receiving less than 400 mm of rainfall per year were limited to the northern part of the basin; however, this area expanded considerably in 2014 and even further in 2019, eventually affecting the majority of the study area. The authors emphasize the importance of understanding this temporal evolution and spatial distribution within the basin.

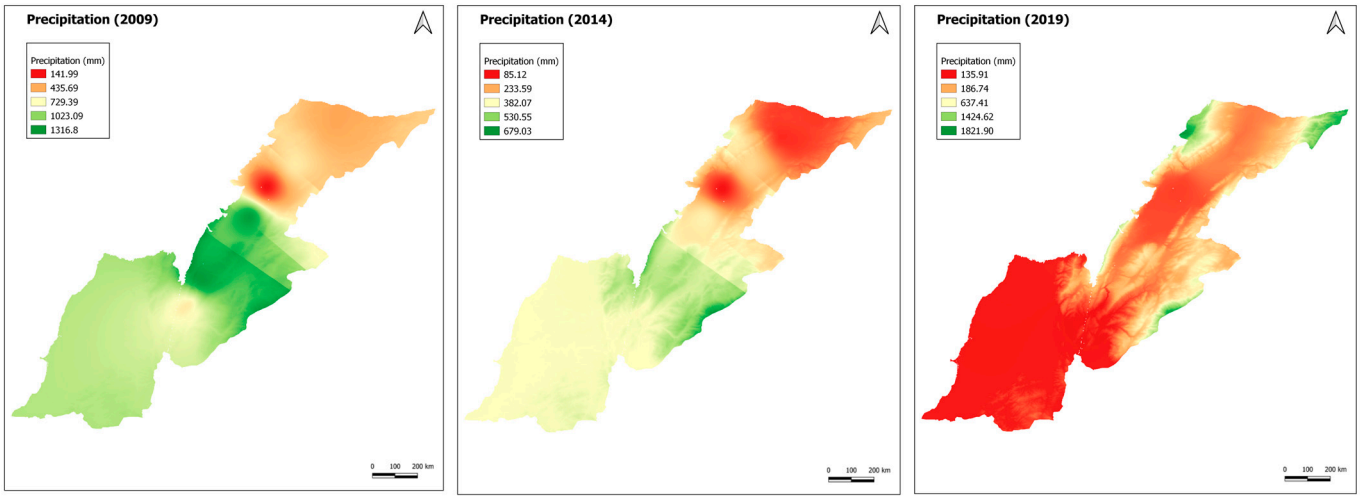

(**a**) (**b**) (**c**)

Figure 4. Spatial distribution of the *precipitation*: (**a**) 2009; (**b**) 2014; (**c**) 2019.

Precipitation distribution across the entire Litani River Basin is as follows: 29.9% of the basin receives between 1000 and 1400 mm/year, 39.4% between 700 and 1000 mm/year, 25.6% between 400 and 700 mm/year, and 5.1% between 300 and 400 mm/year. Due to the semi-arid climate characterizing the southern part of the basin, the evaporation coefficient of the Litani River reaches approximately 68.2% annually (Figure 5). However, this evaporation rate is generally lower during the winter months (Litani River Authority).

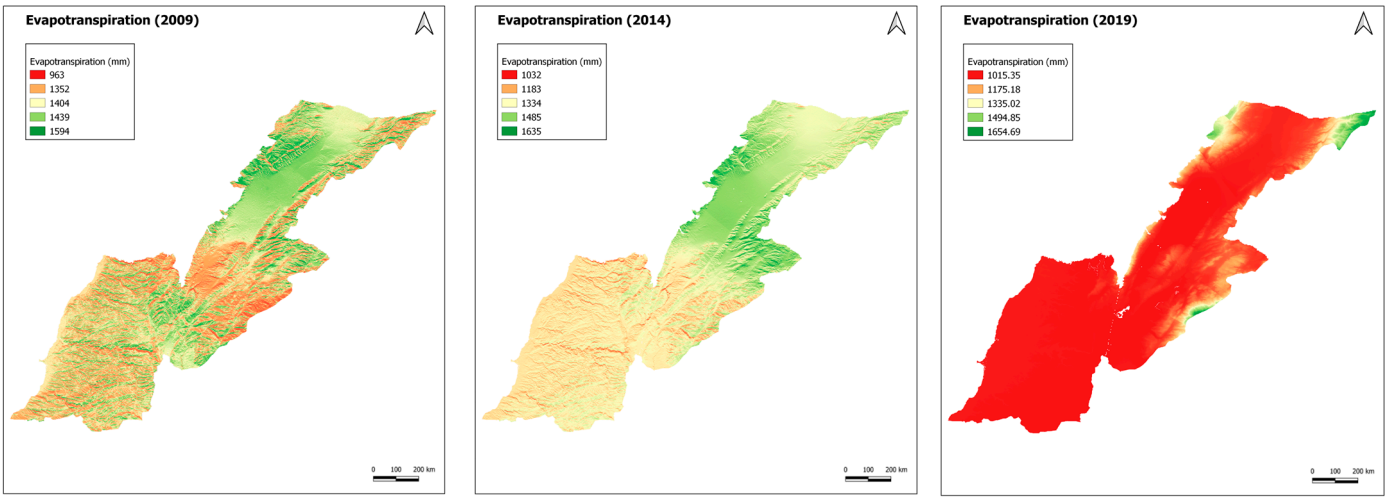

(**a**) (**b**) (**c**)

Figure 5. Spatial distribution of the evapotranspiration: (**a**) 2009; (**b**) 2014; (**c**) 2019.

The *infiltration* rate of *precipitation* into aquifers and adjacent basins varies considerably depending on the geological formations and fault systems present in the watershed.

According to the Litani River Authority, most of the basin's wells are primarily used for domestic purposes, with typical extraction rates ranging from 2000 to 4000 m^3/day.

Analysis of evapotranspiration (Figure 5) and average temperatures (Figure 6) for the years 2009, 2014, and 2019 (Tables 6 and 7) reveals slight increases between the first and third quartiles. Evapotranspiration initially decreased by 4.2% between 2009 and 2014 and then increased by 7.2% between 2014 and 2019. Similarly, average temperatures showed an initial decrease of 6.8% between 2009 and 2014, followed by an increase of 11.2% between 2014 and 2019.

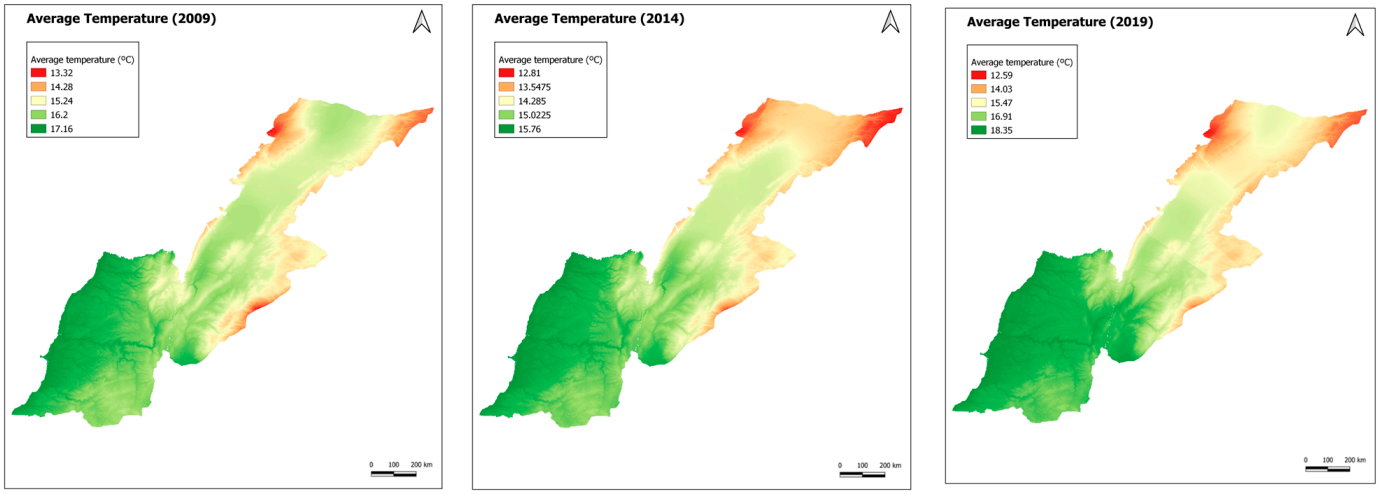

(**a**) (**b**) (**c**)

Figure 6. Spatial distribution of the mean temperatures: (**a**) 2009; (**b**) 2014; (**c**) 2019.

Table 6. Average data of evapotranspiration for 2009, 2014, and 2019 in the study area.

Period (dd/mm/yyyy)	Evapotranspiration (mm)				
	Minimum	1st Quartile	Median	3rd Quartile	Maximum
1 September 2009–31 August 2010	952.78	1352.49	1404.21	1439.09	1595.39
1 September 2013–31 August 2014	998.85	1294.61	1345.12	1418.24	1641.33
1 September 2018–31 August 2019	994.68	1392.97	1442.29	1479.67	1657.37

Table 7. Average data of temperature for 2009, 2014, and 2019 in the study area.

Period (dd/mm/yyyy)	Average Temperature (°C)				
	Minimum	1st Quartile	Median	3rd Quartile	Maximum
1 September 2009–31 August 2010	13.28	15.46	15.91	16.42	17.16
1 September 2013–31 August 2014	12.80	14.29	14.82	15.28	15.77
1 September 2018–31 August 2019	12.56	15.43	16.49	17.69	18.36

3.1.3. Soil

Topographic gradients influence some soil parameters, such as saturated hydraulic conductivity (Figure 7), whereas geological unit segmentation influences others, such as *soil moisture* (Figure 8) and soil depth (Figure 9). The northern and southern west have the lowest saturated hydraulic conductivity of soil in the upper and lowest layers, whereas the central western section and some patches along the eastern half have the highest saturated hydraulic conductivity of soil. The highest n of Van Genuchten values is found in the southeastern and central western parts of the research region, while the lowest values are found in the northeastern and southeastern parts (Figures 7 and 8). The lowest matric

potential values can be found in the southeastern part of the research area, with a few patches in the western central part, while the highest metric potential values can be found in the eastern part (Figures 7–9). Most of the studied region (the central, eastern, and western parts) appears to have a thin second layer of soil (Figure 9). Small spots in the central eastern and southwestern parts of the studied region exhibit high soil second-layer thickness ratings (Figure 9).

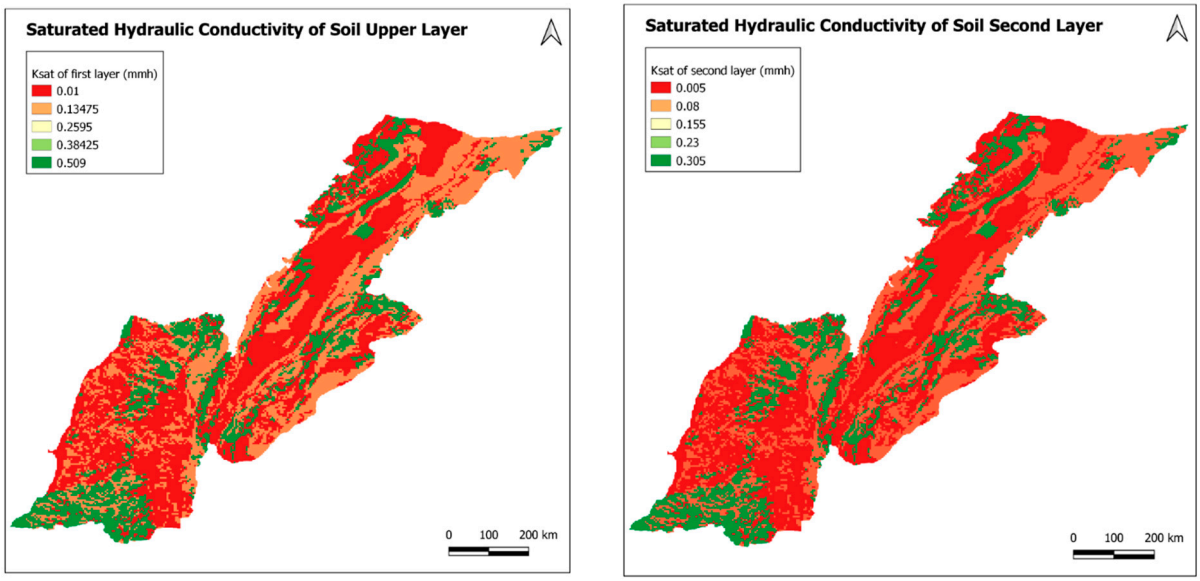

(**a**) (**b**)

Figure 7. Soil parameters of the study area: (**a**) saturated hydraulic conductivity of soil upper layer; (**b**) saturated hydraulic conductivity of soil second layer.

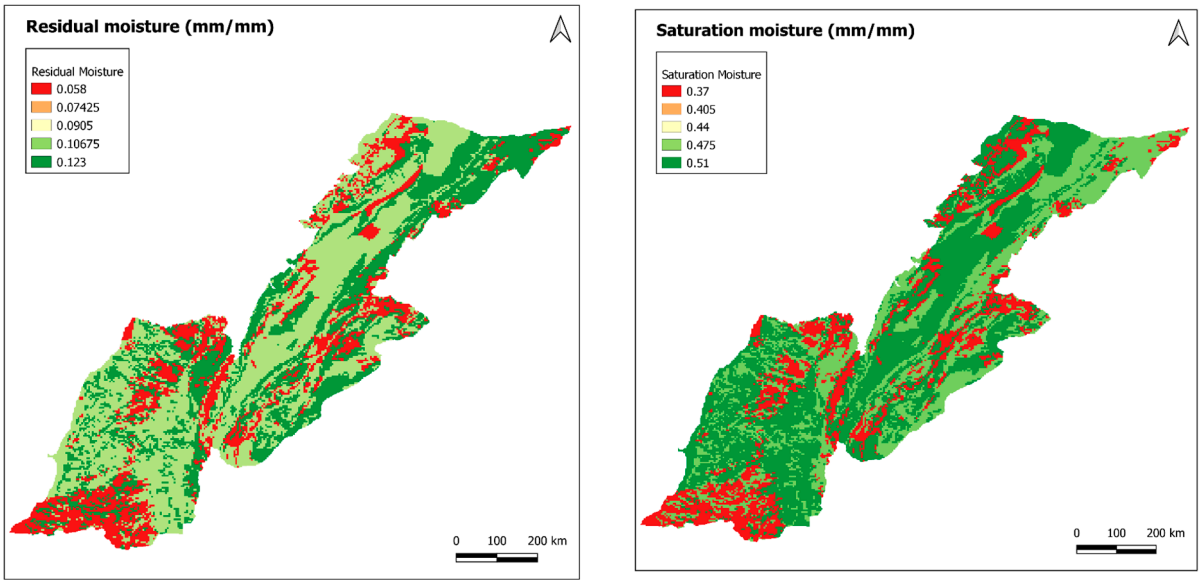

(**a**) (**b**)

Figure 8. Soil properties of the study area: (**a**) residual moisture; (**b**) saturation moisture.

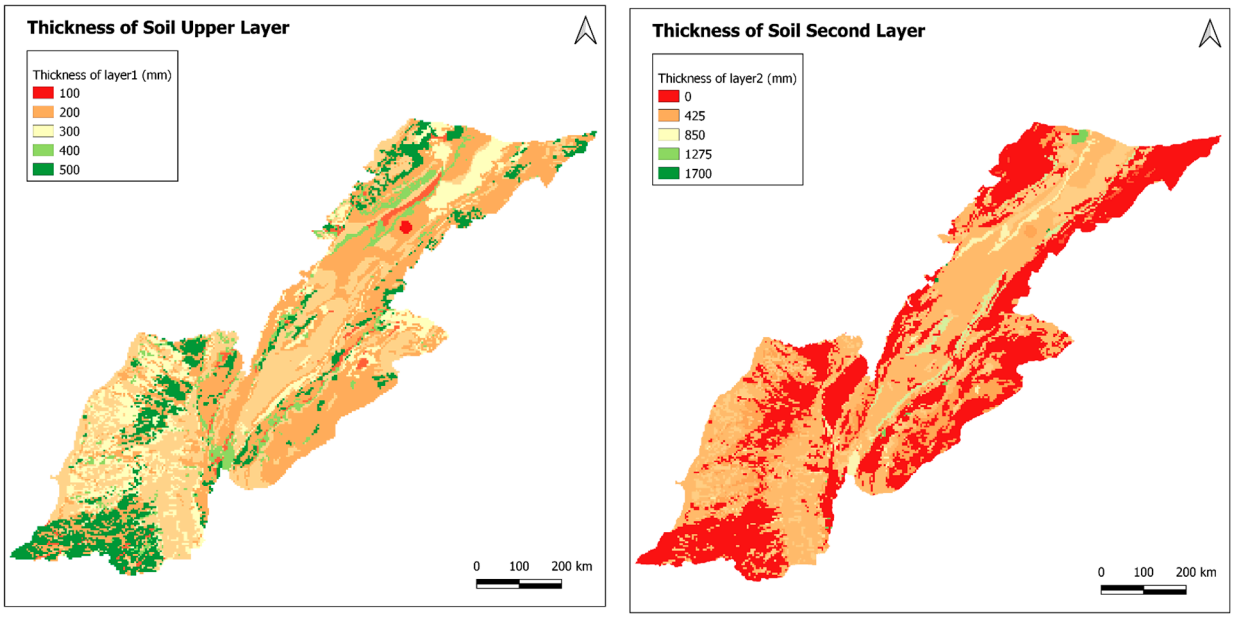

(**a**) (**b**)

Figure 9. Soil properties of the study area: (**a**) thickness of soil upper layer; (**b**) thickness of soil second layer.

3.1.4. Land Cover Change in Litani River Basin

Figure 10 presents the land use in the Litani River Basin. There is no major infrastructure throughout the basin, except for a few tourist-oriented recreational sites located in the lower part of the basin. Water demand for tourism activities during the months of June to September is estimated at approximately 0.08 Mm^3, or approximately 0.008 m^3/s. Furthermore, only one water pumping station for domestic use is located in the basin, with a pumping rate of 18,000 m^3/day (Lebanese Ministry of Energy and Water). The lower basin also supports unevenly distributed agricultural activity, thanks to an irrigation canal that supplies 26 Mm^3 of water to the coastal areas located north and south of the river mouth. In addition, a volume of 13.5 million cubic meters is transferred from Lake Qaraoun to compensate for the water deficit in summer.

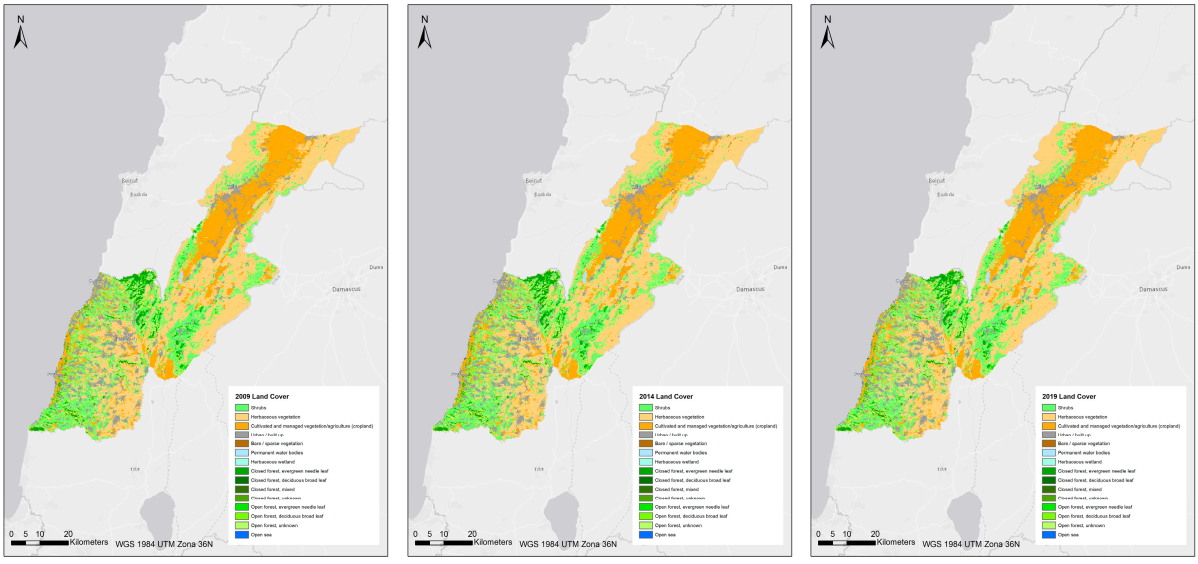

(**a**) (**b**) (**c**)

Figure 10. Land cover map of Litani River Basin: (**a**) 2009; (**b**) 2014; (**c**) 2019.

To more effectively assess land use changes, land cover types were grouped into fifteen final categories: scrub, herbaceous vegetation, cultivated and managed vegetation/agriculture (cropland), urban areas, sparse vegetation, permanent water bodies, herbaceous wetlands, dense evergreen coniferous forests, dense deciduous broadleaf forests, dense mixed forests, unspecified dense forests, open evergreen coniferous forests, open deciduous broadleaf forests, unspecified open forests, and open sea (Table 8).

Table 8. Land cover change in Litani River watershed for the period 2009–2014–2019.

	Areas(ha)				
Land Cover Classes	**2009**	**2014–2009**	**2014**	**2019–2014**	**2019**
Shrubs	92,823.42	−29.28	92,794.14	−796.25	91,997.89
Herbaceous vegetation	152,243.20	−65.11	152,178.09	154.93	152,333.01
Cultivated and managed vegetation/agriculture (cropland)	78,699.41	34.89	78,734.30	442.15	79,176.45
Urban/built up	39,980.06	46.43	40,026.49	136.43	40,162.92
Bare/sparse vegetation	396.63	5.28	401.90	−9.95	391.95
Permanent water bodies	640.10	9.96	650.06	18.05	668.11
Herbaceous wetland	30.31	19.27	49.58	55.99	105.56
Closed forest, evergreen needle leaf	7759.52	0.00	7759.52	−10.84	7748.68
Closed forest, deciduous broad leaf	141.37	0.00	141.37	0.00	141.37
Closed forest, mixed	71.87	0.00	71.87	0.00	71.87
Closed forest, unknown	4605.06	−16.16	4588.90	−3.76	4585.14
Open forest, evergreen needle leaf	4670.46	−2.14	4668.32	−17.55	4650.77
Open forest, deciduous broad leaf	39.90	0.00	39.90	0.00	39.90
Open forest, unknown	22,033.94	−3.98	22,029.96	29.48	22,059.44
Open sea	277.72	0.00	277.72	0.97	278.69

GIS spatial analysis allowed us to track land use changes over a 10-year period, revealing a significant increase in urban areas. A slight increase in agricultural land of approximately 0.044% (or 35 ha) was observed between 2009 and 2014, followed by another modest increase of 0.56% (or +442 ha) between 2014 and 2019. Over the entire period 2009–2019, the cumulative increase reached +477 ha, representing an average annual growth rate of +0.06%. The main irrigated crops in the basin include banana and citrus trees in the coastal areas on both sides of the river, as well as olive trees, fruit trees, and vines.

In addition to agriculture, urban development is also placing increasing pressure on the basin. An increase of +0.11% was recorded between 2009 and 2014, followed by a further increase of +0.34% between 2014 and 2019, representing an annual change of +0.045%, or a total increase of +183 ha over ten years.

Forests (open and closed, evergreen conifers, deciduous broadleaf, mixed, or unspecified) remained broadly stable over the ten years. A slight decrease of −0.06% (−22 ha) was observed between 2009 and 2014, followed by a near-status quo between 2014 and 2019 (−0.007% or −2.7 ha). This stability could be the result of awareness campaigns and strengthened regulations.

The study highlights a significant increase in grassy wetlands: +63.5% between 2009 and 2014 and +113% between 2014 and 2019, representing a total area of 105.56 hectares. These areas play an essential role in riverbank management: they accumulate pollutants, provide a habitat for wildlife, limit bank erosion, and improve water quality and the surrounding landscape.

Among other types of land cover, permanent water bodies recorded an increase of +4.3% over 10 years: +1.55% between 2009 and 2014 and then +2.8% between 2014 and 2019. At the same time, a decrease of −1% (−825.5 ha) in shrubland was observed between 2009 and 2019, while a slight increase of +0.06% (+90 ha) concerned areas of herbaceous

vegetation. Finally, bare land or land with sparse vegetation increased by +1.33% between 2009 and 2014 and then decreased by −2.5% between 2014 and 2019.

3.1.5. Erosion

The map below shows the erosion risk in the Litani River Basin (Figure 11). The erosion risk there varies between very low erosion risk covering over 3.3% of the LRB area, low erosion risk with an area of 5.5%, medium erosion risk for over 59.1% of the LRB area, high erosion risk with an area of 16.9%, and very high erosion risk with an area of 15.1%, with less than 0.04% of urban areas within the LRB.

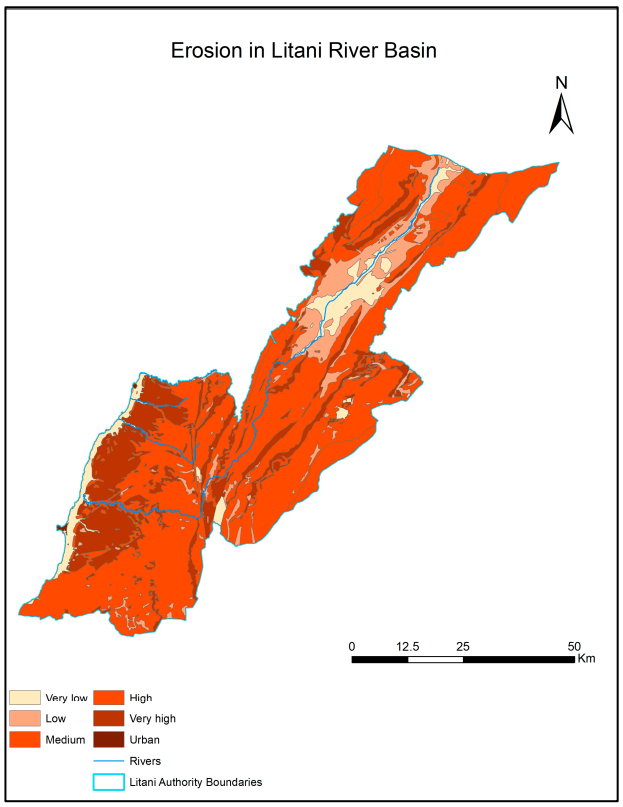

Figure 11. Soil properties of the study area: GIS map showing the erosion intensity in Litani River.

3.2. Hydrological Regime of the Study Area

The WiMMed model generated a series of raster maps with a spatial resolution of 30 × 30 m, corresponding to the various hydrological variables calculated. These variables were produced for each season (fall, winter, spring, and summer) of the years 2009, 2014, and 2019. For their interpretation, the variables were classified into three categories: state variables, intermediate variables, and meteorological variables.

- *Infiltration* (mm) and *runoff* (mm) are considered intermediate variables. Due to the spatial variability of the input data, the model output variables exhibit significant variations from one cell to another within the same image.
- *Soil moisture* in the first and second layers (mm) is classified as a state variable.
- *Precipitation* (mm) and *snowfall* (mm) are treated as meteorological variables.

Comparison of data from 2009, 2014, and 2019 reveals notable changes in soil hydrological parameters in the study region, showing significant variations between these three years. The core of this study is the analysis of the impact of land use changes on the hydrological regime. This link will be examined in detail in the following section. Changes in hydrological variables will be compared for each season, due to the significant variation in

vegetation cover (morphological and physiological) throughout the year: summer, autumn, winter, and spring.

The results indicate a marked difference in *infiltration* (Table 9), particularly in spring, with a reduction of −37% between 2009 and 2014, followed by a further decline of −78% between 2014 and 2019. This represents a total decrease of −86% over ten years, or an average annual decline of −8.6%. These results highlight the complexity of the area's hydrological regime and demonstrate the model's ability to reproduce this spatial variability in calculating the water balance.

Table 9. Average data of *infiltration* (mm) by season for 2009, 2014, and 2019 in the study area.

Season	Autumn			Winter			Spring			Summer		
INFILTRATION	**2009**	**2014**	**2019**	**2009**	**2014**	**2019**	**2009**	**2014**	**2019**	**2009**	**2014**	**2019**
Mean	36.04	7.27	42.6	191.995	105.6	55.78	312.3	196	42.45	312.835	212.49	28.9
Standard Deviation	27.42	4.8	11.51	79.21986	43.6	3.4	0.29569	13.18	9.03	0.04286	0.13	0.8
Maximum	72.08	14.54	58.18	311.85	179.9	56.42	312.75	212.3	55.91	312.91	212.67	30.55
Minimum	0	0	27.24	72.14	15.67	55.15	311.85	179.9	28.99	312.76	212.32	27.3

Runoff in the study area (Table 10) decreased in all seasons between 2009 and 2019. In spring, a reduction of −79% was observed between 2009 and 2014, followed by a further reduction of −36% between 2014 and 2019. This represents a total reduction of −87% over ten years, or an average annual decrease of −8.7%. An exception is noted in autumn, where *infiltration* and *runoff* first decreased between 2009 and 2014 and then increased between 2014 and 2019. Specifically, *infiltration* decreased by −80% between 2009 and 2014, before increasing by +486% between 2014 and 2019. As for *runoff*, a decrease of −97% was observed between 2009 and 2014, followed by a dramatic increase of +947% between 2014 and 2019.

Table 10. Average data of *runoff* (mm) by season for 2009, 2014, and 2019 in the study area.

	Autumn			Winter			Spring			Summer		
RUNOFF	**2009**	**2014**	**2019**	**2009**	**2014**	**2019**	**2009**	**2014**	**2019**	**2009**	**2014**	**2019**
Mean	54.83	1.31	13.71	364.61	62.55	53.27	619.58	129.06	82.005	619.60	135.63	84.89
Standard Deviation	46.07	1.19	11.65	185.29	27.03	14.90	0.01	4.77	1.28	0.005	0.0045	7.15
Maximum	109.66	2.62	27.42	619.56	122.49	79.12	619.6	135.63	84.89	619.61	135.64	84.89
Minimum	0	0	0	109.66	2.62	27.42	619.56	122.49	79.12	619.6	135.63	84.89

Regarding *soil moisture* in the first layer (Table 11, Figure 12), slight decreases were observed between 2009 and 2019: −8% in autumn and −32% in winter. Conversely, a slight increase was noted in spring (+5%) and summer (+1.8%).

Table 11. Average data of *soil moisture* of the first layer (mm) by season for 2009, 2014, and 2019 in the study area.

	Autumn			Winter			Spring			Summer		
SOIL MOISTURE FIRST LAYER	**2009**	**2014**	**2019**	**2009**	**2014**	**2019**	**2009**	**2014**	**2019**	**2009**	**2014**	**2019**
Mean	54.805	32.34	45.11	92.13	67.1	62.7	52.34	55.6	54.95	28.39	29.8	28.9
Standard Deviation	18.57	3.4	11.5	18.03	14.71	3.4	12.75	12.18	58.92	0.59	1.13	0.83
Maximum	82.37	37.45	63	124.51	99.1	70.41	75.14	78.9	56.93	29.41	32.03	30.55
Minimum	27.24	27.24	27.24	59.76	35.25	55.15	29.54	32.27	1.37	27.38	27.64	27.3

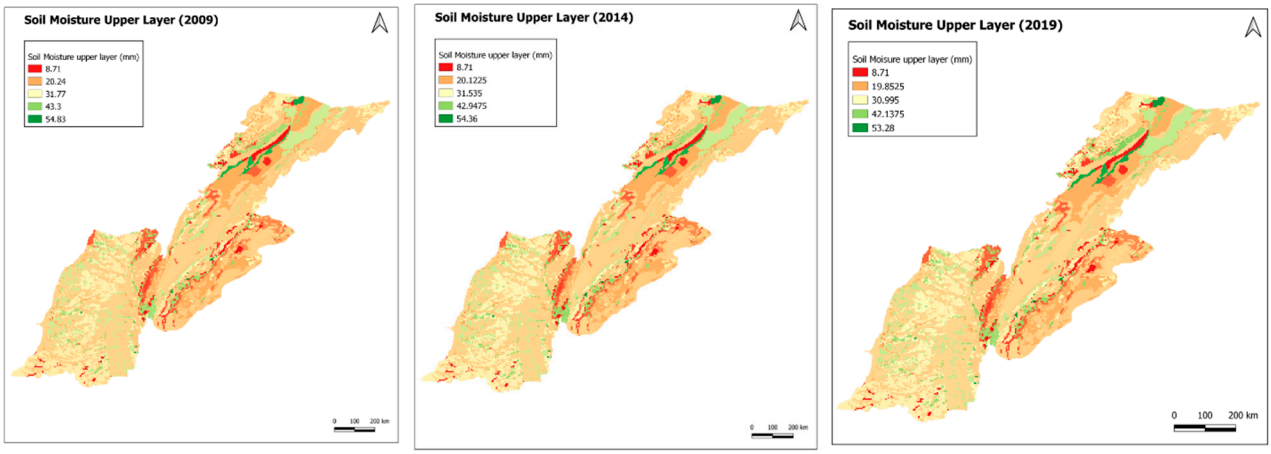

(**a**) (**b**) (**c**)

Figure 12. Spatial distribution of the *soil moisture* of the first layer depending on the season: (**a**) 2009; (**b**) 2014; (**c**) 2019.

The hydrological regime of the second soil layer (Table 12, Figure 13) shows a generalized decrease in moisture in all seasons over the ten-year period: −18% in autumn, −31% in winter, −36% in spring, and −32% in summer.

Table 12. Average data of *soil moisture* of the second layer (mm) by season for 2009, 2014, and 2019 in the study area.

	Autumn			**Winter**			**Spring**			**Summer**		
SOIL MOISTURE SECOND LAYER	**2009**	**2014**	**2019**	**2009**	**2014**	**2019**	**2009**	**2014**	**2019**	**2009**	**2014**	**2019**
Mean	41.38	31.2	33.8	68.84	60.6	47.2	88.61	88.6	56.9	80.83	85.4	54.65
Standard Deviation	6.81	0.08	1.59	14.39	16.9	5.52	4.19	1.58	1.37	0.62	0.39	0.15
Maximum	51.67	31.34	36.6	95.42	89.9	57.6	95.26	91.1	58.9	81.88	86.13	54.93
Minimum	31.09	31.09	31.09	42.26	31.35	36.8	81.97	86.19	54.9	79.79	84.72	54.3

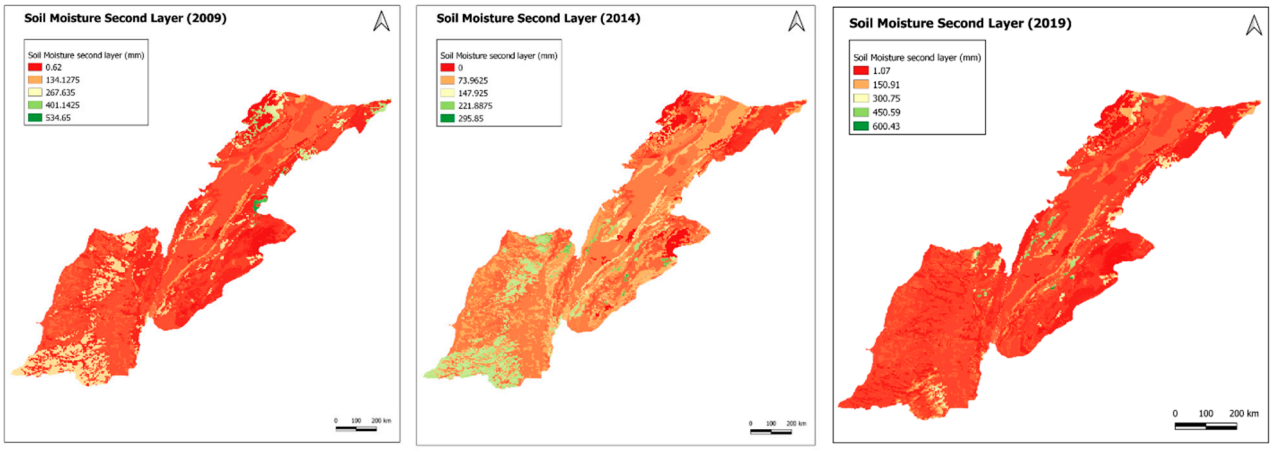

(**a**) (**b**) (**c**)

Figure 13. Spatial distribution of *soil moisture* of the second layer depending on the season: (**a**) 2009; (**b**) 2014; (**c**) 2019.

The seasonal variation in *precipitation* (Table 13, Figure 4) and *snowfall* (Table 14, Figure 14) is clearly visible. The region's strong seasonality is demonstrated by the almost

complete absence of rainy episodes during the summer. The majority of *snowfall* in winter is concentrated at the highest elevations of the study area (Figure 14).

Table 13. Average data of rainfall during 2009, 2014, and 2019 in the study area.

Period (dd/mm/yyyy)	Precipitation (mm)				
	Minimum	1st Quartile	Median	3rd Quartile	Maximum
1 September 2009–31 August 2010	141.89	633.37	896.58	945.23	1318.28
1 September 2013–31 August 2014	84.80	311.66	384.13	400.66	682.45
1 September 2018–31 August 2019	135.89	186.74	637.41	1424.62	1821.90

Table 14. Average data of *snowfall* during 2009, 2014, and 2019 in the study area.

Period (dd/mm/yyyy)	Snowfall (mm)				
	Minimum	1st Quartile	Median	3rd Quartile	Maximum
1 September 2009–31 August 2010	3.98	7.82	13.10	28.93	288.55
1 September 2013–31 August 2014	0.58	32.89	34.22	37.98	125.21
1 September 2018–31 August 2019	0.00	9.05	29.89	24.99	73.62

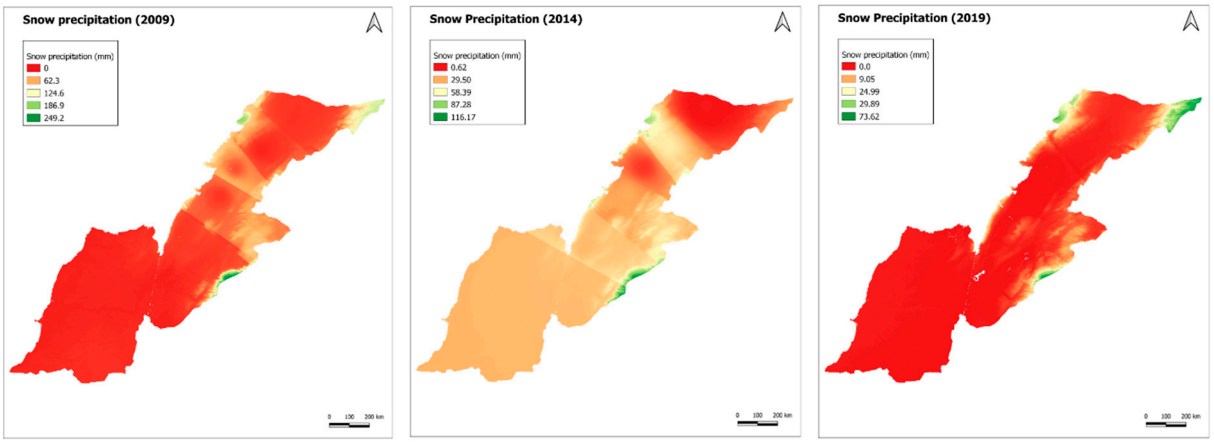

(**a**) (**b**) (**c**)

Figure 14. Spatial distribution of the *snowfall*: (**a**) 2009; (**b**) 2014; (**c**) 2019.

A slight increase in *precipitation* and *snowfall* was also observed between the first and third quartiles for the years 2009, 2014, and 2019. This is explained by an overall decrease in *precipitation* of −28% between 2009 and 2019. More specifically, a sharp decrease of −57% was recorded between 2009 and 2014, followed by an increase of +66% between 2014 and 2019. When comparing the first and third quartiles, an increase of +49% was observed in 2009, +28% in 2014, and +663% in 2019, the latter representing the largest increase.

Regarding *snowfall*, an overall increase of +128% is recorded over the ten years between 2009 and 2019. This change includes an increase of +161% between 2009 and 2014, followed by a slight decrease of −13% between 2014 and 2019. Between the first and third quartiles, the data reveal an increase of +270% in 2009, +15% in 2014, and +176% in 2019, thus illustrating the seasonal variability of *snowfall* during the period studied.

3.2.1. Impact of Climate Change on Hydrological Variables of the Litani River Basin, Lebanon

In this study, the scenarios for the year 2040 are as follows: in the RCP 2.6 scenario, this study anticipates a 2 °C increase in temperature and a 10% decrease in *precipitation* in the Litani River Basin region. The second scenario, RCP 8.5, anticipates a 5 °C increase in temperature in the study area, as well as a 20% reduction in *precipitation*. The findings revealed

that the impact of future climate change on hydrological variables in the research area varies seasonally, since the RCP scenarios are directly related to the rainfall and *precipitation* rates. The differences between the *precipitation*, evapotranspiration, *snowfall*, and temperature are revealed by comparing the current rates, as demonstrated in Figures 14 and 15, with those of the projected scenarios RCP 2.6 and RCP 8.5 (Figures 15–18).

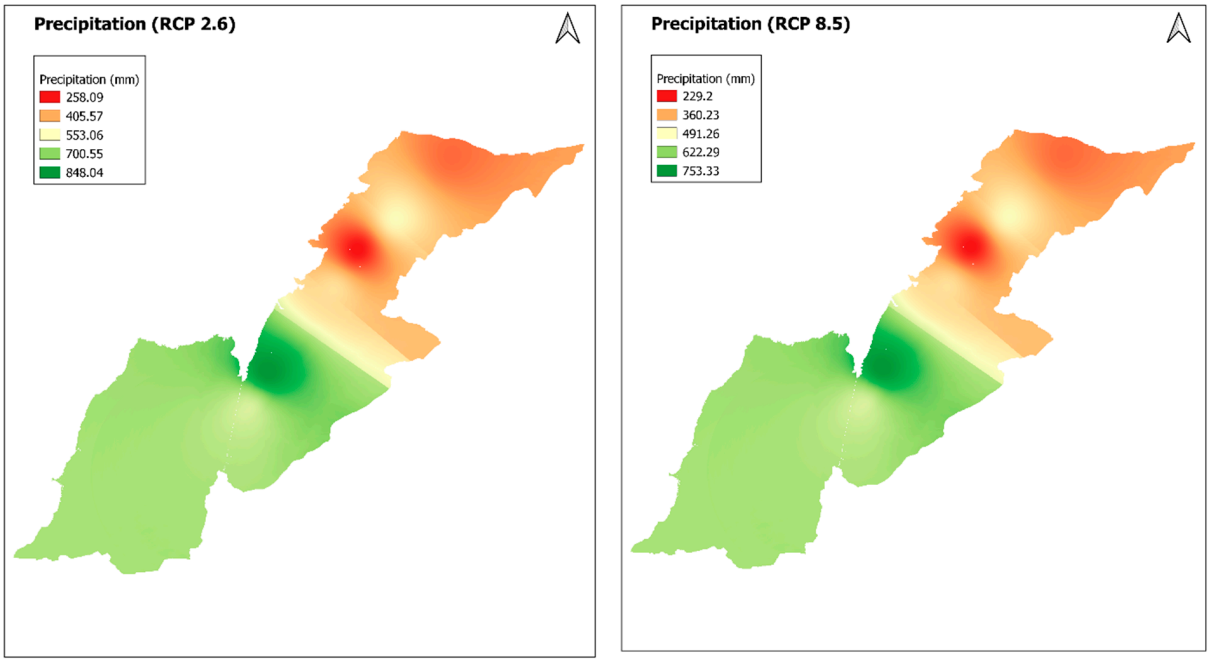

(**a**) (**b**)

Figure 15. Simulation of the total rainfall in the study area: (**a**) for scenario RCP 2.6; (**b**) for scenario RCP 8.5.

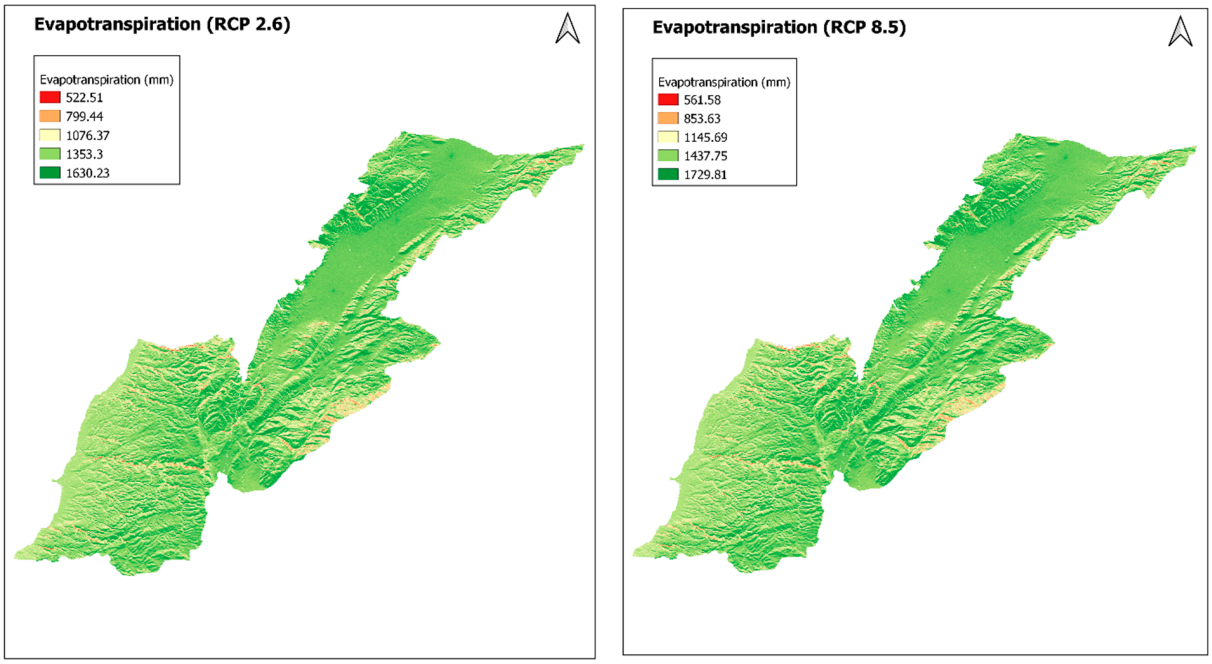

(**a**) (**b**)

Figure 16. Simulation of the total evapotranspiration in the study area: (**a**) for scenario RCP 2.6; (**b**) for scenario RCP 8.5.

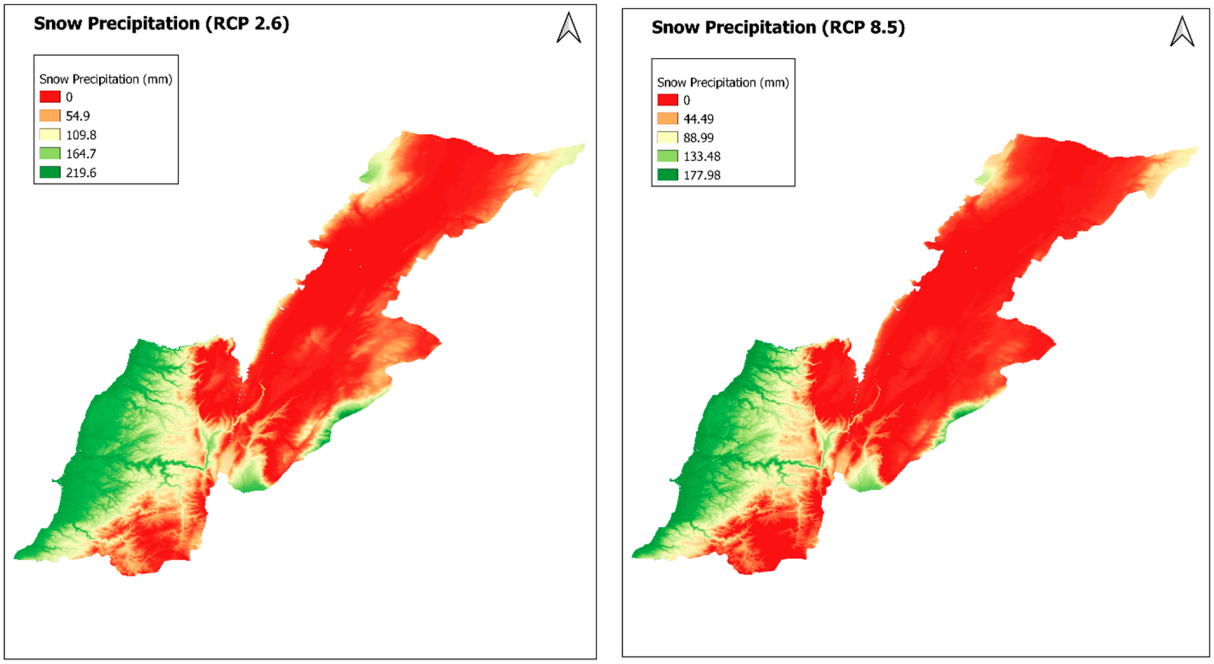

(**a**) (**b**)

Figure 17. Simulation of the total *snowfall* in the study area: (**a**) for scenario RCP 2.6; (**b**) for scenario RCP 8.5.

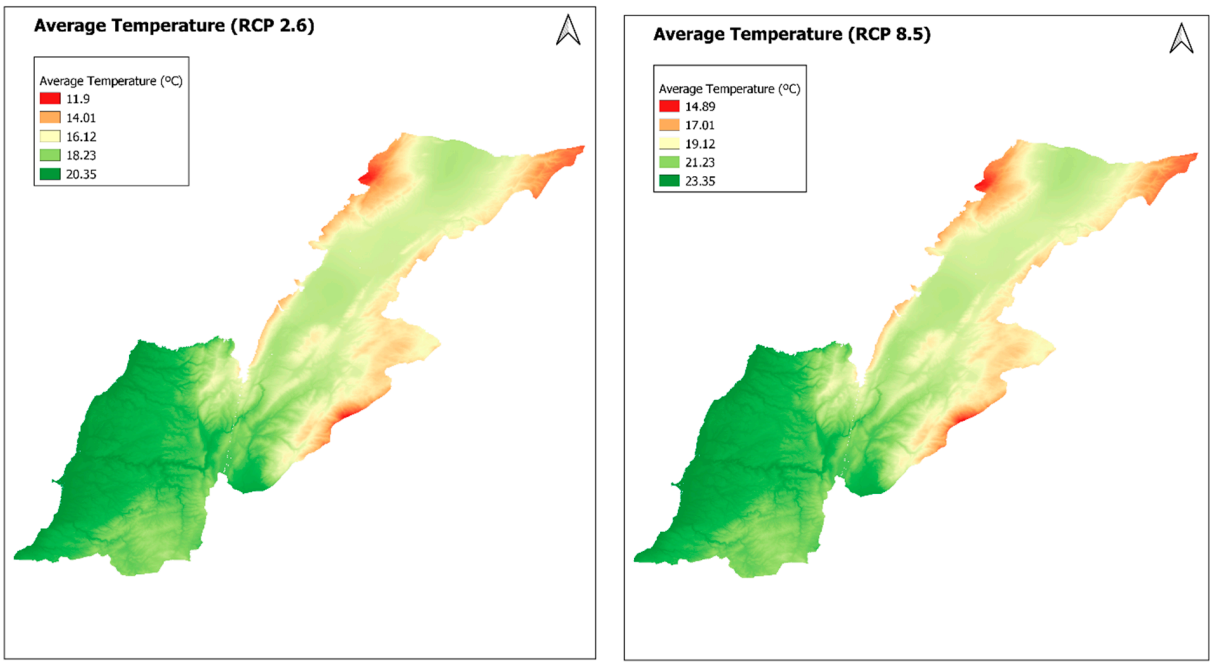

(**a**) (**b**)

Figure 18. Simulation of the temperature in the study area: (**a**) for scenario RCP 2.6; (**b**) for scenario RCP 8.5.

3.2.2. *Infiltration* and *Runoff*

As shown in Table 15, the average *infiltration* (Figure 19) and *runoff* (Figure 20) values in 2019 were 186.9 mm and 390.8 mm, respectively. Compared with the 2019 baseline year, future climate scenarios show a marked decline in the hydrological regime. Under the RCP 2.6 scenario, *infiltration* decreases by −33.4% and *runoff* by −89.1%. Under the RCP 8.5 scenario, the decline reaches −47.9% for *infiltration* and −93.6% for *runoff*.

Table 15. Hydrological regime yearly average variable for the control year 2019 and climatic change scenarios (RCP 2.6 and RCP 8.5) of the Litani River Basin area.

	(mm)					
	Infiltration	**Runoff**	**Snowfall**	**Rainfall**	**Soil Moisture 1**	**Soil Moisture 2**
2019	186.9	390.8	29.89	637.41	52.7	54.4
RCP2.6	124.5	42.7	5.2	585.6	58.6	58.68
RCP8.5	97.4	25.2	3.52	520.2	55.4	51.5

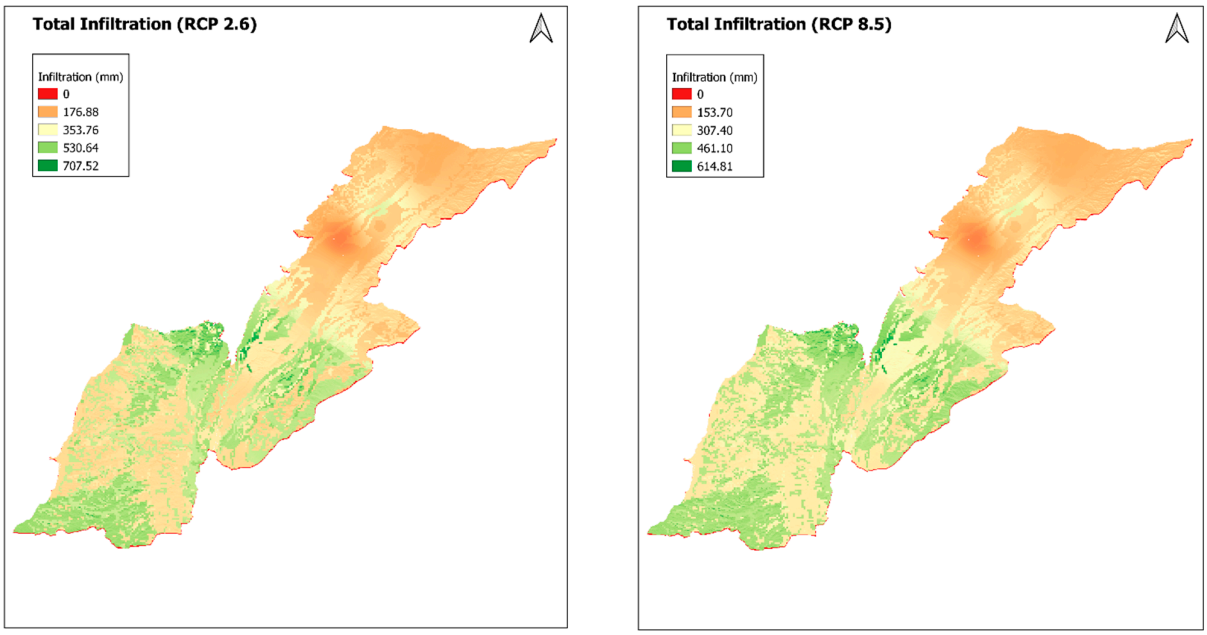

(**a**) (**b**)

Figure 19. Simulation of total soil *infiltration* in the study area: (**a**) for scenario RCP 2.6; (**b**) for scenario RCP 8.5.

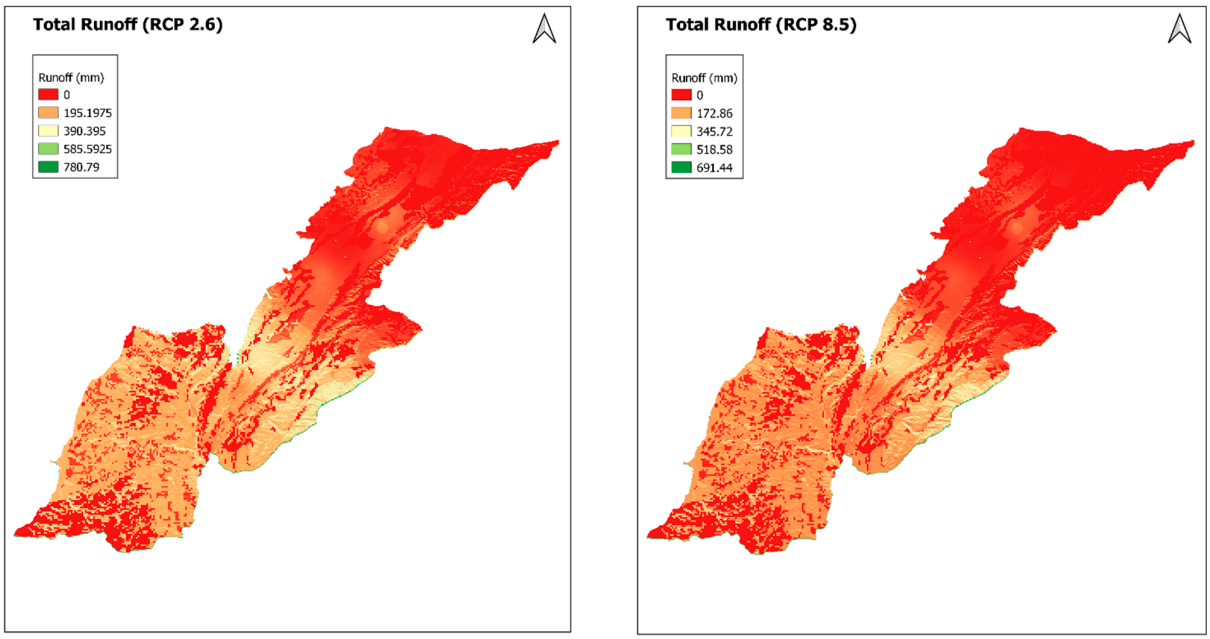

(**a**) (**b**)

Figure 20. Simulation of total *runoff* in the study area: (**a**) for scenario RCP 2.6; (**b**) for scenario RCP 8.5.

Soil moisture in the second layer was 54.4 mm in 2019. It shows a slight increase under the RCP 2.6 scenario, reaching 58.68 mm, an increase of +7.9% compared to 2019. In contrast, it decreases to 51.5 mm under RCP 8.5, which corresponds to a decrease of −5.3% compared to the base year.

For the fall 2019 season, *infiltration* and *runoff* values (Table 16) were 41.48 mm and 32.99 mm, respectively. When comparing future scenarios to 2019, *infiltration* decreases by −48.6% under RCP 2.6 and −54.9% under RCP 8.5. *Runoff* decreases by −96.18% under RCP 2.6 and by −97.9% under RCP 8.5.

Table 16. Hydrological regime average variable of the study area in autumn under control year and climatic change scenarios.

	(mm)					
	Infiltration	**Runoff**	**Snowfall**	**Rainfall**	**Soil Moisture 1**	**Soil Moisture 2**
2019	41.84	32.99	NA	NA	50.47	38.1
RCP2.6	21.52	1.26	8.1	181.8	68.48	40.18
RCP8.5	18.86	0.69	1.8	64.5	64.31	38.17

In spring 2019, both scenarios also show a decrease in *infiltration* and *runoff*. *Infiltration* decreases by −32.8% under RCP 2.6 and by −39.18% under RCP 8.5, while *runoff* decreases by −89% under RCP 2.6 and by −92.5% under RCP 8.5 (Table 16).

3.2.3. *Soil Moisture*

In autumn, the *soil moisture* layer 1 (Table 16, Figure 21) showed an increase in 2019 by +135.7% in the RCP 2.6 case and an increase in the RCP 8.5 case in 2019 by +27.4%. The percentage of increase in *soil moisture* layer 2 (Table 16, Figure 22) in the two scenarios is smaller than the increase shown in *soil moisture* layer 1. We state a +5.45% under RCP 2.6 and a +0.18% under RCP 8.5 compared to *soil moisture* layer 2 in 2019 (38.1 mm).

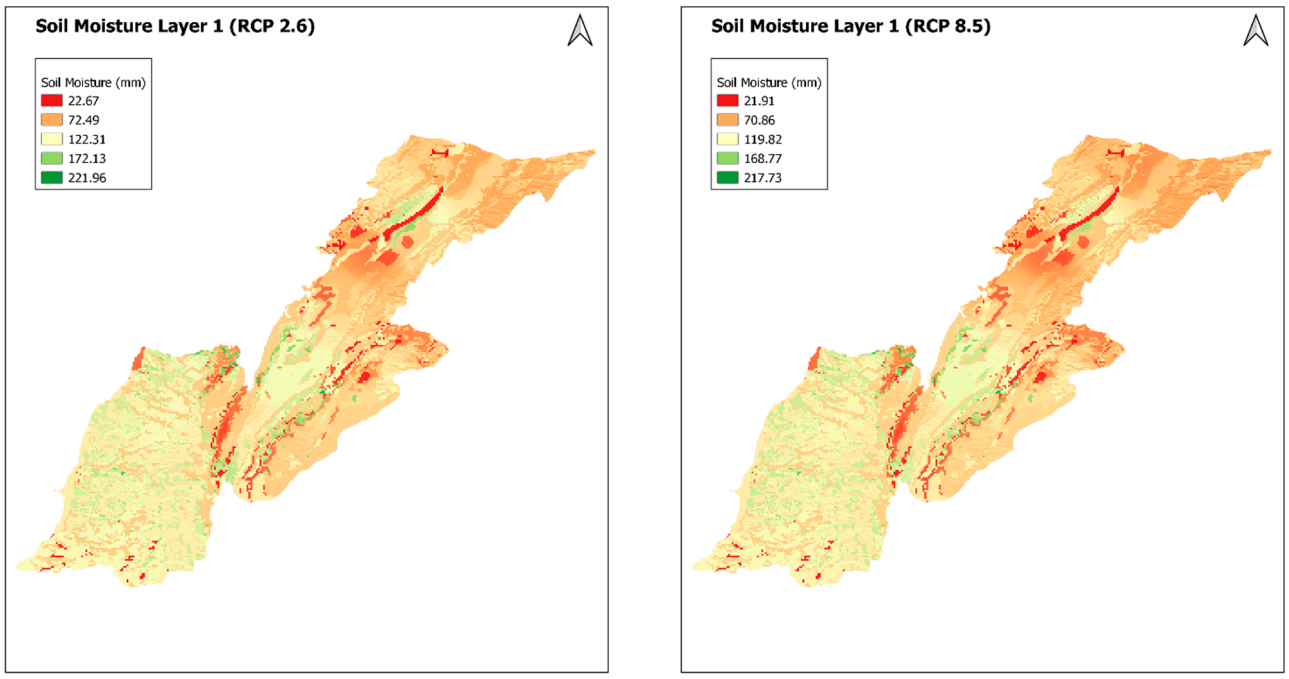

(**a**) (**b**)

Figure 21. Simulation of total *soil moisture* layer 1 in the study area: (**a**) for scenario RCP 2.6; (**b**) for scenario RCP 8.5.

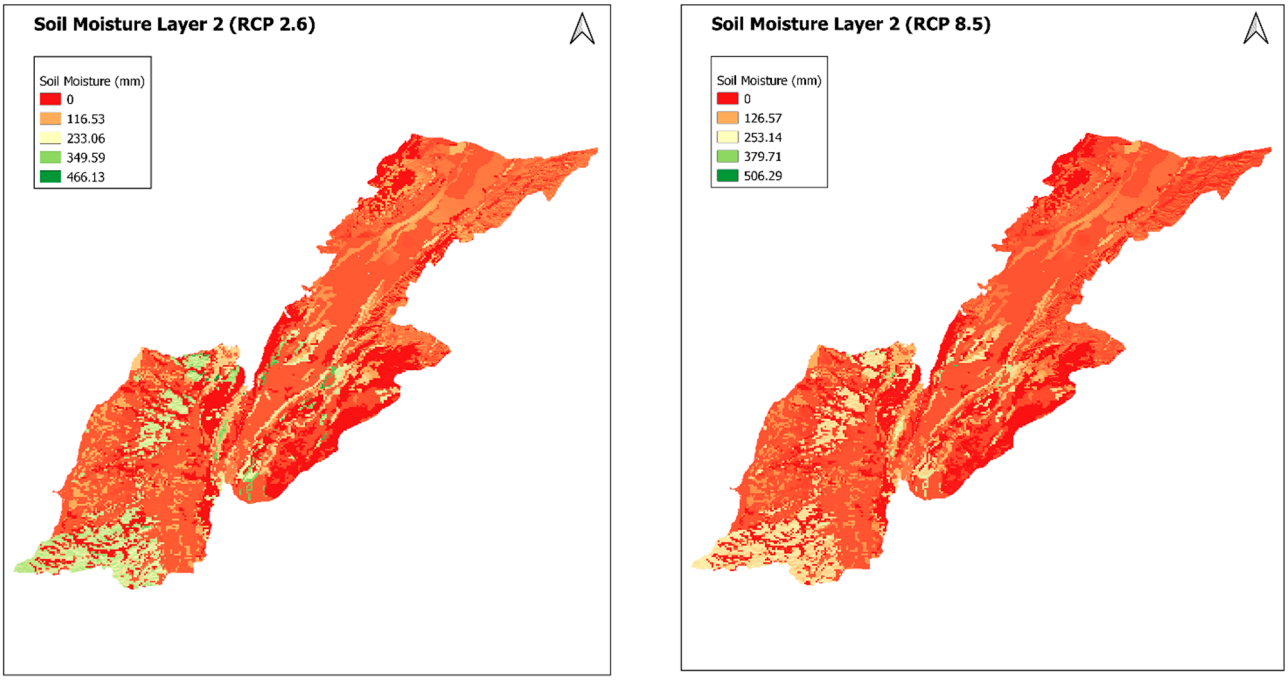

(**a**) (**b**)

Figure 22. Simulation of total *soil moisture* layer 2 in the study area: (**a**) for scenario RCP 2.6; (**b**) for scenario RCP 8.5.

Concerning *soil moisture* layer 1 and 2 in the spring season (Table 17), the results mention a decrease by −13.25% in RCP 2.6 for the *soil moisture* layer 1, referring to spring 2019 values, and a decrease by −19% in RCP 8.5. An increase is shown in scenario RCP 2.6 for the *soil moisture* layer 2 by +3.9% and a slight decrease by −6.2% in RCP 8.5. In summer, soil moisture layer 1 shows a slight increase under both RCP2.6 and RCP8.5 scenarios based on 2019, while the soil moisture layer 2 exhibits a decrease under RCP8.5 compared to 2019 (Table 18). In winter, soil moisture layer 1 shows an increase under both scenarios, while soil moisture layer 2 remains stable under RCP2.6 compared to 2019 and decreases under RCP8.5 (Table 19).

Table 17. Hydrological regime average variable of the study area in spring under control year and climatic change scenarios.

	(mm)					
	Infiltration	**Runoff**	**Snowfall**	**Rainfall**	**Soil Moisture 1**	**Soil Moisture 2**
2019	289.43	641.01	NA	NA	50.71	67.63
RCP2.6	194.48	70.60	5.4	61.2	43.99	70.27
RCP8.5	176.01	47.91	1.31	18.83	41.06	63.42

Table 18. Hydrological regime average variable of the study area in summer under control year and climatic change scenarios.

	(mm)					
	Infiltration	**Runoff**	**Snowfall**	**Rainfall**	**Soil Moisture 1**	**Soil Moisture 2**
2019	237.01	516.19	NA	NA	26.75	52.23
RCP2.6	202.3	70.95	0	6.3	28.17	65.05
RCP8.5	121.55	32.11	0.17	3.33	27.48	50.39

Table 19. Hydrological regime average variable of the study area in winter under control year and climatic change scenarios.

	(mm)					
	Infiltration	**Runoff**	**Snowfall**	**Rainfall**	**Soil Moisture 1**	**Soil Moisture 2**
2019	180.4	370.92	NA	NA	83.7	59.66
RCP2.6	79.58	28.17	48.6	377.1	93.81	59.23
RCP8.5	73.25	20.09	10.8	92.75	88.8	54.18

4. Discussion

Extensive research exists about the impact of land cover alterations on watershed dynamics and water resources, particularly in Mediterranean regions where ecosystems are more susceptible to anthropogenic and climatic changes [47,48]. In the Litani River Basin (LRB), alterations in land use and land cover in recent decades, primarily due to inadequate land management and urban expansion, have significantly impacted the region's water balance. Changes in land cover and climate may have both immediate and long-term effects on terrestrial hydrology, altering the balance between rainfall and evapotranspiration [17,19]. Land cover change has the potential to affect a variety of natural and biological processes, including soil nutrients, *soil moisture*, soil erosion, and land productivity [21]. It also affects hydrological processes, including the *infiltration* rates, *runoff*, and evapotranspiration in river basins, all of which are important for crop development and vegetation regeneration [22]. This study employed the WIMMED model to examine the impact of land cover alterations on water flow in the years 2009, 2014, and 2019, with projected climate change scenarios (RCP 2.6 and RCP 8.5) from 2019 to 2040. This research indicates that alterations in land cover, including deforestation and agricultural expansion, are intricately associated with fluctuations in *infiltration*, *runoff*, and *soil moisture*. *Soil moisture* is the volume of water in soil layer 1 (0–7 cm, the surface is at 0 cm). The volumetric soil water is associated with the soil texture (or classification), soil depth, and the underlying groundwater level. The documented reduction in forest cover (−24.7 ha) and the increase in agricultural (+477 ha) and developed areas (+183 ha) correspond with regional patterns of land conversion in Mediterranean watersheds, which are linked to reduced *infiltration* and heightened surface *runoff* [49,50]. Forests enhance soil permeability, capture *precipitation*, and regulate evapotranspiration. These are all elements that are forfeited when trees are felled. Removing them typically deteriorates soil quality, impedes water retention, and increases the risk of flooding [51,52]. Research in Lebanon and adjacent nations has demonstrated that the expansion of agricultural and urban regions frequently results in soil compaction, an increased susceptibility to erosion, and alterations in natural hydrological patterns [53,54].

Our findings confirm the principal concepts of prior studies on regional hydrology. Zabaleta et al. (2014) demonstrated that the conversion of forested areas to agricultural land in the Basque Country resulted in increased *runoff* and decreased *infiltration*, corroborating the findings of our model in the LRB [55]. The loss of vegetation might increase variability in seasonal *runoff* and decrease *soil moisture* in response to rising temperatures [56], as evidenced in our RCP 8.5 projections. Climate models indicate that, in the Litani River watershed, both RCP 2.6 and RCP 8.5 will result in a significant reduction in *infiltration* and *runoff*, with RCP 8.5 leading to a more pronounced decline. This aligns with studies indicating that elevated temperatures and less *precipitation* in Mediterranean basins enhance evapotranspiration and diminish soil water content [57,58]. The anticipated *infiltration* reductions of up to 20% under RCP 8.5 parallel the *infiltration* losses identified by Milly et al. (2005) and others for semi-arid basins in comparable warming scenarios [59].

The reduction in *soil moisture*, particularly in the second layer, is critical for the health of ecosystems and agriculture. This study demonstrates that reduced *soil moisture* results in diminished plant growth, lower agricultural yields, and an increased risk of droughts [60,61]. The second layer of *soil moisture* remains steady for a brief period annually under RCP 2.6, indicating its capacity to withstand moderate climatic change. This stability diminishes under the more severe RCP 8.5 scenario, which forecasts temperature rises above 5 °C, aligning with IPCC findings [62].

These findings indicate that altering land utilization, disregarding climate forecasts, significantly impacts *infiltration* and *soil moisture* levels. This corroborates the findings of Muñoz-Villers and McDonnell (2013): in disturbed environments, land cover exerts a greater influence on watershed-scale hydrological flows than short-term climate variability [63]. These concepts indicate the necessity for watershed management strategies that integrate land use planning and climate adaptation. Mitigating further deforestation, promoting green infrastructure, and rehabilitating degraded land will alleviate the adverse effects of hydrological disruption and ensure the long-term health of the LRB and other Mediterranean basins. This study provides valuable insights; nonetheless, it has specific limitations, including the utilization of identical soil data throughout all years and the formulation of assumptions in the RCP scenarios. Dynamic soil mapping, enhanced groundwater modeling, and validation with empirical hydrological data could all contribute to future endeavors. Incorporating social and economic aspects into land use estimates would enhance the realism of the scenarios.

5. Conclusions

Our study demonstrates that climate change and land use trends have a critical impact on water resources and soil quality in the Litani River Basin (LRB). In a context of increasing global water scarcity, Lebanon must urgently adopt practical and strategic actions to preserve its ecosystems and ensure water supply [64,65]. The Mediterranean region is particularly vulnerable, subject to increasing water stress due to erratic rainfall, rising temperatures, and ever-increasing water demand, which threatens food security, biodiversity, and sustainable development.

In this study, the distributed hydrological model WiMMed was used to analyze a set of topographic, meteorological, soil, and geological data for the years 2009, 2014, and 2019. The model generated hydrological variables through raster maps, providing a physical representation of the basin's water balance. The integration of projections from global climate models (GCMs) made it possible to anticipate future hydrological scenarios between 2019 and 2040.

The results obtained allow several specific conclusions to be drawn based on the observed values:

- A marked reduction in *infiltration* was observed in spring, with a decrease of −86% over ten years (2009–2019).
- *Runoff* decreased by −87% over the same period, particularly in spring and winter.
- *Soil moisture* in the second layer recorded a continuous decline of up to −36% depending on the season.
- Under the RCP scenarios, *infiltration* could further decrease by −33.4% to −47.9%, while *runoff* could fall by −89.1% to −93.6%.
- *Soil moisture* in the second layer could increase by +7.9% under RCP 2.6 but decrease by −5.3% under RCP 8.5.

These results reveal that, in a changing climate, decreases in *soil moisture* and *runoff* will have major consequences for agriculture, ecosystems, and water resources. This underscores the urgent need to implement adaptive policies that take into account both RCP 8.5

(catastrophic) and RCP 2.6 (more moderate) scenarios to ensure the sustainable availability of water resources. Understanding the spatio-temporal dynamics of watersheds is essential for effective freshwater management, now and in the future. Furthermore, this study highlights that land use changes have a more pronounced effect on *soil moisture* (second layer) than climate variations themselves. This observation reinforces the importance of integrated and proactive land management. It is crucial that policymakers promote the preservation of natural ecosystems, reforestation, and riverbank restoration to maintain ecological balance. The projected reduction in surface *runoff* has mixed effects: while it reduces the risk of water erosion, it increases the risk of wind erosion on parched soils. A decrease in *soil moisture* in the second layer limits water availability for plants, disrupts microbial communities, alters nutrient cycles, and increases vulnerability to droughts. Targeted ecological riverbank restoration can help improve water quality, reduce crop contamination, enhance the region's attractiveness, and promote groundwater recharge.

Applying these findings to water resources planning in Lebanon, particularly in the Litani Basin, will help guide strategies and policies toward effective adaptation to climate change. Priority must be given to integrated water resource management, ecosystem protection, and the promotion of sustainable development practices to ensure a resilient and sustainable future for the region.

Supplementary Materials: The following supporting information can be downloaded at: https://www.mdpi.com/article/10.3390/f16091461/s1, Table S1: Thickness of upper layer 1 and lower layer 2 from the soil map of Lebanon at 1:50,000 scale database.

Author Contributions: Conceptualization, G.P.-R. and G.K.; methodology, G.P.-R. and S.K.; formal analysis, G.K. and G.P.-R.; investigation, G.K., G.P.-R. and S.K.; resources, G.P.-R.; data curation, G.P.-R., G.K. and S.K.; writing—original draft preparation, G.K., G.P.-R. and S.K.; writing—review and editing, G.P.-R., G.K. and S.K.; supervision, G.P.-R. and S.K.; funding acquisition, G.P.-R. and G.K. All authors have read and agreed to the published version of the manuscript.

Funding: This research was funded by the Spanish Agency for International Development Cooperation (AECID) under the MAEC-AECID Scholarship Program for citizens of Africa and the Middle East, within the framework of the AFRICA-MED Program, academic year 2022–2023, grant number BDNS 603057.

Data Availability Statement: Data are contained within the article.

Acknowledgments: The authors would like to thank the researchers of the ERSAF group (PAI RNM360) of the University of Cordoba for their unconditional support of this work, as well as the Spanish Agency for International Development Cooperation for their financial support.

Conflicts of Interest: The authors declare no conflicts of interest.

References

1. Dlamini, N.S.; Kamal, M.R.; Bin Mohd Soom, M.A.; Faisal bin Mohd, M.S.; Bin Abdullah, A.F.; Sai Hin, L. Modeling Potential Impacts of Climate Change on Streamflow Using Projections of the 5th Assessment Report for the Bernam River Basin, Malaysia. *Water* **2017**, *9*, 226. [CrossRef]
2. Yan, D.; Werners, S.; Ludwig, F.; Huang, H.Q. Hydrological response to climate change: The Pearl River, China under different RCP scenarios. *J. Hydrol.* **2015**, *4*, 228–245. [CrossRef]
3. Dudgeon, D.; Arthington, A.H.; Gessner, M.O.; Kawabata, Z.-I.; Knowler, D.J.; Lévêque, C.; Naiman, R.J.; Prieur-Richard, A.-H.; Soto, D.; Stiassny, M.L.J.; et al. Freshwater biodiversity: Importance, threats, status and conservation challenges. *Freshw. Biol.* **2006**, *81*, 163–182. [CrossRef]
4. Durance, I.; Ormerod, S.J. Trends in water quality and discharge confound long-term warming effects on river macroinvertebrates. *Freshw. Biol.* **2009**, *54*, 388–405. [CrossRef]
5. IPCC. The Physical Science Basis. In *Working Group, I Contribution to the Fifth Assessment Report of the Intergovernmental Panel on Climate Change*; Cambridge University Press: Cambridge, UK, 2013.

6. Fowler, H.; Blenkinsop, S.; Tebaldi, C. Linking climate change modeling to impacts studies: Recent advances in downscaling techniques for hydrological modeling. *Int. J. Climatol.* **2007**, *27*, 1547–1578. [CrossRef]
7. Loaiciga, H.A.; Valdes, J.B.; Vogel, R.; Garvey, J.; Schwarz, H. Global warming and the hydrologic cycle. *J. Hydrol.* **1996**, *174*, 83–127. [CrossRef]
8. Diep, L.; Hayward, T.; Walnycki, A.; Husseiki, M.; Karlsson, L. *Water, Crises and Conflict in MENA: How Can Water Service Providers Improve Their Resilience?* IIED working paper; IIED: London, UK, 2017.
9. Tejerina-Garro, F.L.; Maldonado, M.; Ibañez, C.; Pont, D.; Roset, N.; Oberdorff, T. Effects of natural and anthropogenic environmental changes on riverine fish assemblages: A framework for ecological assessment of rivers. *Braz. Arch. Biol. Technol.* **2005**, *48*, 91–108. [CrossRef]
10. Arab Water Council. Vulnerability of arid and semi-arid regions to climate change–impact and adaptive strategies. In Proceedings of the 5th World Water Forum, Istanbul, Turkey, 16–22 March 2009.
11. Midgley, S.; Dejene, A.; Mattick, A. *Adaptation to Climate Change in Semi-Arid Environments Experience and Lessons from Mozambique*; FAO: Rome, Italy, 2012.
12. Gebremicael, T.G.; Mohamed, Y.A.; Van der Zaag, P. Attributing the hydrological impact of different land use types and their long-term dynamics through combining parsimonious hydrological modeling, alteration analysis and PLSR analysis. *Sci. Total Environ.* **2019**, *660*, 1155–1167. [CrossRef]
13. Dwarakish, G.S.; Ganasri, B.P. Impact of land use change on hydrological systems: A review of current modeling approaches. *Cogent Geosci.* **2015**, *1*, 1115691. [CrossRef]
14. LARI. *Lebanese Agricultural Research Center-Climatic Data*; Daily Bulletin: Ontario, CA, USA, 2018.
15. FAO. *Soil Tillage in Africa: Needs and Challenges*; FAO Soils Bulletin 69; Soil Resources, Management and Conservation Service, Land and Water Development Division; FAO: Rome, Italy, 1993.
16. Tavakoli, M.; De Smedt, F. Impact of climate change on streamflow and *soil moisture* in the Vermilion Basin, Illinois. *J. Hydrol.* **2011**, *17*, 1059–1070. [CrossRef]
17. Pérez, J.R.; Rebollo, F.J.; Castaño, S.; Rodríguez-Díaz, J.A. A distributed hydrological model for Mediterranean environments: WiMMed. In Proceedings of the MODSIM09 International Congress on Modelling and Simulation, Cairns, Australia, 13–17 July 2009; pp. 3500–3506.
18. Ruiz-Pérez, G.; Castaño, S.; Rebollo, F.J.; Rodríguez-Díaz, J.A. Use of WiMMed model to evaluate water balance in the Almanzora basin under current and future scenarios. *Cuad. Investig. Geográfica* **2019**, *45*, 655–679.
19. Li, K.Y.; Coe, M.T.; Ramankutty, N.; De Jong, R. Modeling the hydrological impact of land-use change in West Africa. *J. Hydrol.* **2007**, *337*, 258–268. [CrossRef]
20. Sharif, J.R.; Khosravi, H.; Alamdarlou, E.S. Assessment the effects of land use changes on soil physicochemical properties in Jafarabad of Golestan province, Iran. *Bull. Env. Pharmacol. Life Sci.* **2014**, *3*, 296–300.
21. Chen, F.; Peng, B. The effects of land use changes on soil conditions in arid region. *Chin. Geogr. Sci.* **2000**, *10*, 226–230. [CrossRef]
22. Niu, C.Y.; Musa, A.; Liu, Y. Analysis of *soil moisture* condition under different land uses in the arid region of Horqin sandy land northern China. *Solid Earth* **2015**, *6*, 1157–1167. [CrossRef]
23. Nazarenko, L.; Schmidt, G.A.; Miller, R.L.; Tausnev, N.; Kelley, M.; Ruedy, R.; Russell, G.L. Future Climate Change under RCP Emission Scenarios with GISS Model E2. *J. Adv. Model. Earth Syst.* **2015**, *7*, 244–267. [CrossRef]
24. Basheer, A.K.; Lu, H.; Omer, A.; Ali, A.B.; Abdelgader, A. Impacts of climate change under CMIP5 RCP scenarios on the streamflow in the Dinder River and ecosystem habitats in Dinder National Park, Sudan. *Hydrol. Earth Syst. Sci.* **2016**, *20*, 1331–1353. [CrossRef]
25. Xu, C.Y. Climate change and hydrologic models: A review of existing gaps and recent research developments. *Water Resour. Manag.* **1999**, *13*, 369–382. [CrossRef]
26. Prudhomme, C.; Jakob, D.; Svensson, C. Uncertainty and climate change impact on the flood regime of small UK catchments. *J. Hydrol.* **2003**, *277*, 1–23. [CrossRef]
27. Shaban, A. Analyzing climatic and hydrologic trends in Lebanon. *J. Environ. Sci. Eng.* **2011**, *5*, 483–492.
28. IDRC; CNRS-L; LRA; DSA. *Towards an Ecosystem Approach to the Sustainable Management of the Litani Watershed*; Technical Report; Cadham Hayes Systems: Ottawa, ON, Canada, 2007; p. 143.
29. Jomaa, I.; Shaban, A. Improving water-Use efficiency and productivity in the Litani River Basin. In *The Litani River, Lebanon: An Assessment and Current Challenges*; Shaban, A., Hamzé, M., Eds.; Water Science and Technology Library; Springer: Berlin/Heidelberg, Germany, 2018; Volume 85, pp. 107–117. [CrossRef]
30. Mcheik, A.; Awad, A.; Fadel, A.; Mounzer, C.; Nasreddine, S. Effect of irrigation water quality on the microbial contamination of Fresh vegetables in the Bekaa Valley, Lebanon. *Am. J. Agric. For.* **2018**, *6*, 191–197.
31. Nehme, N.; Haidar, C. The Physical, Chemical and Microbial Characteristics of Litani River Water. In *The Litani River, Lebanon: An Assessment and Current Challenges*; Springer: Berlin/Heidelberg, Germany, 2018; p. 179.

32. Shaban, A.; Hamzé, M. (Eds.) *The Litani River, Lebanon: An Assessment and Current Challenges*; Water Science and Technology Library; Springer: Cham, Switzerland, 2018; Volume 85.
33. Herrero, J.; Millares, A.; Aguilar, C.; Egüen, M.; Losada, M.A.; Polo, M.J. Coupling Spatial and Time Scales in The Hydrological Modeling of Mediterranean Regions. In Proceedings of the WiMMed 11th International Conference on Hydroinformatics, CUNY Academic Works, New York, NY, USA, 17–21 August 2014.
34. Egüen, M.; Aguilar, C.; Herrero, J.; Millares, A.; Polo, M.J. On the influence of cell size in physically based distributed hydrological modeling to assess extreme values in water resource planning. *Nat. Hazards Earth Syst. Sci.* **2012**, *12*, 1573–1582. [CrossRef]
35. Herrero, J.; Polo, M.J.; Moñino, A.; Losada, M.A. An energy balance snowmelt model in a Mediterranean site. *J. Hydrol.* **2009**, *371*, 98–107. [CrossRef]
36. Van Vuuren, D.P.; Stehfest, E.; den Elzen, M.G. RCP2.6: Exploring the possibility to keep global mean temperature increase below 2 °C. *Clim. Change* **2011**, *109*, 95. [CrossRef]
37. Aguilar, C.; Polo, M.J.; Herrero, J.; Losada, M. WiMMed, a distributed physically based watershed model (II): Application examples. In *Environmental Hydraulics: Theoretical, Experimental and Computational Solutions*; Taylor and Francis Group: London, UK, 2010; pp. 29–30.
38. Aguilar, C. Efectos de Escala en Procesos Hidrológicos. Aplicación a la Cuenca del río Guadalfeo (Granada). Ph.D. Thesis, University of Cordoba, Córdoba, Spain, 2008.
39. Darwish, T. *Soil Map of Lebanon at 1/50000*; Centre National de la Recherche Scientifique-Centre de télédetection: Beirut, Lebanon, 2006.
40. FAO. *World Reference Base for Soil Resources*; Food and Agriculture Organization of the United Nations: Rome, Italy, 1998; Volume 3.
41. Saxton, K.E.; Rawls, W.J. Soil Water Characteristic Estimates by Texture and Organic Matter for Hydrologic Solutions. *Soil Sci. Soc. Am. J.* **2006**, *70*, 1569–1578. [CrossRef]
42. Leij, F.J.; Alves, W.J.; van Genuchten, M.T.H.; Williams, J.R. *The UNSODA Unsaturated Hydraulic Database*; EPA/600/R-96/095; U.S. Environmental Protection Agency: Cincinnati, OH, USA, 1996.
43. Litani River Authority (LRA). *Litani River Basin Management Plan*; Litani River Authority (LRA): Khalde, Lebanon, 2015.
44. Darwish, T.; Atallah, T.; Francis, R.; Rizk, C. *Land degradation in Lebanon*; National Council for Scientific Research: Beirut, Lebanon, 2008.
45. United Nations Development Programme (UNDP). *Assessment of Land Degradation Hotspots in the Litani River Basin*; UNDP: Beirut, Lebanon, 2014.
46. Polo, M.J.; Herrero, J.; Pimentel, R.; Pérez-Palazón, M.J. The Guadalfeo Monitoring Network (Sierra Nevada, Spain): 14 years of measurements to understand the complexity of snow dynamics in semiarid regions. *Earth Syst. Sci. Data Discuss.* **2018**, *11*, 154–196. [CrossRef]
47. Allen, R.G.; Pereira, L.S.; Raes, D.; Smith, M. *Crop Evapotranspiration: Guidelines for Computing Crop Water Requirements*; FAO Irrigation and Drainage Paper 56; FAO: Rome, Italy, 1998.
48. Shaban, A.; Khawlie, M.; Abdallah, C. Use of remote sensing and GIS to determine recharge potential zones: The case of Lebanon. *Hydrogeol. J.* **2004**, *12*, 103–111. [CrossRef]
49. Kosmas, C.; Danalatos, N.G.; López-Bermúdez, F.; Romero Díaz, M.A. The effect of land use on soil erosion and land degradation under Mediterranean conditions. In *Mediterranean Desertification: A Mosaic of Processes and Responses*; Geeson, N.A., Brandt, C.J., Thornes, J.B., Eds.; John Wiley & Sons: Sussex, England, 2002; pp. 57–70.
50. Gritti, E.S.; Smith, B.; Sykes, M.T. Vulnerability of Mediterranean basin ecosystems to climate change and invasion. *Glob. Ecol. Biogeogr.* **2006**, *15*, 145–157. [CrossRef]
51. Bonan, G.B. Forests and climate change: Forcings, feedbacks, and the climate benefits of forests. *Science* **2008**, *320*, 1444–1449. [CrossRef]
52. Prospero, J.M.; Lamb, P.J. African droughts and dust transport to the Caribbean: Climate change implications. *Science* **2003**, *302*, 1024–1027. [CrossRef]
53. Saad, S.; Kazpard, V.; Faour, G. Urban sprawl and soil sealing in the Litani River Basin. *Environ. Monit. Assess.* **2021**, *193*, 242.
54. Doummar, J.; Geyer, T.; Noedler, K.; Sauter, M. Estimation of water balance components of a Mediterranean catchment utilizing hydrological modeling and a GIS-based approach. *Hydrol. Process.* **2012**, *26*, 1633–1645.
55. Zabaleta, A.; Martínez de Arano, I.; Uriarte, A. Effect of land use change on *runoff* generation in a small forested watershed. *J. Hydrol.* **2014**, *519*, 1067–1074.
56. Tague, C.; Choate, J.; Grant, G.E. Parameterizing climate impacts on streamflow across a range of mountain basins. *Hydrol. Earth Syst. Sci.* **2013**, *17*, 309–326.
57. Giorgi, F.; Lionello, P. Climate change projections for the Mediterranean region. *Glob. Planet. Change* **2008**, *63*, 90–104. [CrossRef]
58. Vicente-Serrano, S.M.; Lopez-Moreno, J.I. Hydrological response to different land cover and climate scenarios in a Mediterranean catchment. *Hydrol. Process.* **2006**, *20*, 3621–3634.
59. Milly, P.C.D.; Dunne, K.A.; Vecchia, A.V. Global pattern of trends in streamflow and water availability in a changing climate. *Nature* **2005**, *438*, 347–350. [CrossRef] [PubMed]
60. Rockström, J.; Falkenmark, M.; Lannerstad, M.; Karlberg, L. The planetary water boundary: Towards sustainable water use in agriculture. *Front. Ecol. Environ.* **2012**, *10*, 491–497.

61. D'Odorico, P.; Bhattachan, A.; Davis, K.F.; Ravi, S.; Runyan, C.W. Global desertification: Drivers and feedbacks. *Adv. Water Resour.* **2013**, *51*, 326–344. [CrossRef]
62. IPCC. *Sixth Assessment Report–Working Group I: The Physical Science Basis*; IPCC: Geneva, Switzerland, 2021.
63. Muñoz-Villers, L.E.; McDonnell, J.J. Land use change effects on *runoff* generation in a humid tropical montane cloud forest region. *Hydrol. Earth Syst. Sci.* **2013**, *17*, 3543–3560. [CrossRef]
64. UN Water. *World Water Development Report 2024: Water and Climate Change*; UNESCO: Paris, France, 2024.
65. FAO. *AQUASTAT Country Profile: Mediterranean Region*; Food and Agriculture Organization: Rome, Italy, 2023.

Disclaimer/Publisher's Note: The statements, opinions and data contained in all publications are solely those of the individual author(s) and contributor(s) and not of MDPI and/or the editor(s). MDPI and/or the editor(s) disclaim responsibility for any injury to people or property resulting from any ideas, methods, instructions or products referred to in the content.